THE ROLE OF SENESCENCE IN LUNG DISEASES

Masters by Research 2015-2016

Word Count: 7321

Navin Kumar Balagopal (PGR)
150668284

Supervisors: Dr. J Passos, Dr. J Birch and A Lagnado

Abstract

Cellular senescence is a state whereby somatic cells irreversibly cease to proliferate and exhibit various phenotypic changes. Induction of DNA damage response is the most common reason for cellular senescence. Prior work has characterised cellular senescence as a strong target for various age-related diseases. Hence, its role in age-related lung diseases is of particular interest. Two of the highly prevalent age-related lung diseases include COPD and asthma making them an ideal candidate for this study. A distinct characteristic of senescent cells is telomere dysfunction assessed by co-localization between DNA damage response proteins such as γ-H2A.X and telomeres named telomere-associated DNA damage foci (TAF) which can be visualized by Immuno-FISH. The aim of the current project was to identify whether COPD disease severity correlates with TAF levels and if smoke mice exposed mice (COPD model) show similar changes. The second part of the study was to determine whether investigate whether MPC1 might be a marker for senescence. TAF data was also generated for patients with asthma and on mixed allergen-exposed mice (asthma model) to study disease-dependent changes in TAF. The current study shows that TAF levels and induced cellular senescence are associated with COPD pathology and indicates a similar trend might be followed in case of asthma. It also reveals that mouse models of the lung diseases do not reflect the respective phenotypic changes seen in humans. MPC1 protein shows promise as a new marker for senescence though further work is required.

Word count: 241

Contents

List of Tables and Figures

List of Abbreviations

COPD : Chronic Obstructive Pulmonary Disease

DAPI : 4',6-diamidino-2-phenylindole

DDR : DNA Damage Response

Immuno-FISH : Immuno-Fluorescence in situ Hybridisation

IHC: Immunohistochemistry

IPF: Idiopathic Pulmonary Fibrosis

RNA : ribonucleic acid

ROS : reactive oxygen species

SASP : senescence-associated secretory phenotype

SSC : saline sodium citrate

TAF : telomere-associated foci

MA: mixed allergen

MPC1: Mitochondrial Pyruvate Carrier 1

WT : wild type

y-H2AX : phosphorylated histone 2A.X

PBS : phosphate-buffered saline

PFA: paraformaldehyde

M.O.M kit: Mouse on Mouse immunodetection kit

CDC: Centre for disease control

NIH: National institute of health USA

GINA/GIFA: Global initiative for asthma

GOLD: Global initiative for chronic obstructive lung disease

FEV1: Forced expiratory volume in1 second

FVC: Forced vital capacity

TCA cycle: Tricarboxylic acid cycle

Introduction

1.1 Cellular Senescence

The idea of cellular senescence as a mechanism underlying the ageing process dates back to more than half a century ago when Hayflick and Moorhead discovered that healthy cells can only be passaged for a limited number of times before they underwent a halt of proliferation and might be the cause of ageing. This property of cells was described as cellular senescence, and it referred to the distinct process of permanent cell cycle arrest and cessation of proliferation in somatic cells [1]. This hypothesis was further expanded upon and senescence was considered and later proven to be an anti-cancer mechanism that still lead to other diseases[2]. However, senescence itself can be a part of various pathologies as well and has been implicated in many of non-pathological age-dependent diseases and disorders [3].

1.2 Mechanism of cellular senescence induction

The factors that induce cellular senescence include DNA-Damage[4], Telomere damage[5], oncogene-induced senescence[6], chromatin changes[7] and various other stresses. Persistent activation of DNA-Damage and telomere damage pathways are probably the most common reason senescent phenotypes that persist in a cell [8]. A DNA Damage Response (DDR) at the telomeres is induced due to either excessive shortening [9], oxidative damage [5] or loss of shelterin- proteins that are involved in the stabilisation of the telomere structure [10] damage [11] or after dysfunction[10] [12]. DDR is a signalling cascade, characterised by recruitment and modification of proteins at the site of DNA damage. DDR usually begins when cytotoxic stress is experienced. The result of this is activation of damage sensor complexes (ATR and ATM kinases) [13] which induce phosphorylation of histone proteins such as histone 2A.X (γ-H2AX). These reinforce the DNA damage response and converge on the downstream proteins, such as p53 and kinase inhibitor (CDKI), downstream of p53[14]. This prevents the cell from entering S-phase through phosphorylation suppression and inactivation of retinoblastoma protein (pRB) and halting cell proliferation through inhibition of the activation of E2F, a transcription factor required for the expression of cell-cycle progression[15]. A similar outcome may also involve p16 pathway, another CDK inhibitor [15]. On failure to trigger DNA replication and up-regulating cell-cycle inhibitors provoke irreversible termination of cell proliferation that happens in G1 phase[15].

These senescent cells then secrete a cocktail of cytokines, chemokines, growth factors, proteases, and other tissue remodelling factors referred collectively termed as senescence-associated secretory phenotype (SASP) [16] , [7]. The SASP can stabilise senescence in an autocrine manner [17], but also include senescence in surrounding cells in a paracrine manner [18]. The cytokines and chemokines that comprise the SASP include among others Il-6, IL-8, tumour necrosis factor alpha (TNF-α), transforming growth factor beta (TGF-β), chemokine (C-X-C motif) ligand1 (CXCL1), CXCL2, CXCL5 and insulin growth factor (IGF). SASP has been implicated in the infiltration of immune cells, promotion of cancer progression and tissue damage [16].SASP can also trigger chronic inflammation through the activation of nuclear factor kappa-light-chain-enhancer of activated B cells (NF-κB) [19]. This chronic inflammatory response gives prolonged and overly activated immune cells along with morphological and histological changes that occur with an accumulation of senescent cells and this is thought to contribute to age-related diseases[20].

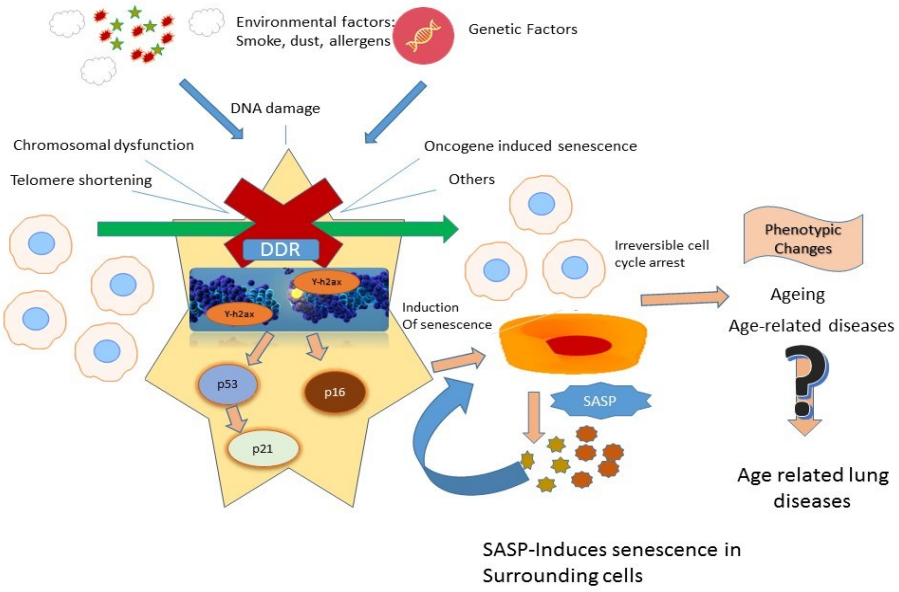

Figure 1: Induction of senescence: Various insults such as telomere damage and oxidative stress, trigger a DNA damage response and elicit cellular senescence through activation of protein cascades involving the cyclin-dependent kinase inhibitors p21 and p16. As a consequence, several features of cellular senescence arise, such as flattened and enlarged cell sizes and the development of an associated pro-inflammatory secretory phenotype, known as the senescence-associated secretory phenotype (SASP), which further induces senescence in adjacent cells. All of which together contribute to the ageing process and development of age-related disease.

1.3 Role of Cellular senescence in respiratory diseases

The respiratory system is essential for delivering oxygen to the body and for maintaining homoeostasis through exhalation of CO_2 and for regulation of internal pressure, temperature and pH. Lungs are the core organ of this system and not only does it have a respiratory function of oxygen absorption and CO_2 release from the blood [21] . It also acts as a means to maintain humidity and temperature while acting as a biochemical and antibacterial/viral barrier and against the various pathogens in the environment. Thus, lung disease hampers respiratory function severely and can often prove fatal. As regions of high oxidative stress and exposure to environmental hazards, lungs particularly are vulnerable to ROS attack and other environmental stress which can induce senescence [22]. Thus senescence is considered a significant factor in the manifestation of lung disease and has already been shown to play a role in other age-related lung diseases. Two of the most common diseases of the lung include asthma and COPD. The incidence of chronic respiratory disease increases with age and senescence has been implicated in a number of age-related lung diseases, namely COPD and ageing markers can be found to increase in Clara cells, predecessor of lung airway epithelium, indicating defected repair process and aggravating inflammation to contribute in the accelerated ageing in the lungs of patients with COPD[20], which result in alveolar destruction and airway destruction due to unsuccessful lung tissue maintenance and remodelling [23]. Along with the complex dysfunction and deterioration of the immune system in ageing population (immunosenescence) [24] induction of senescence in lungs may contribute to the increased incidence of lung diseases in the older population [25].

1.4 COPD and Asthma

The two most common diseases of the lungs are COPD and Asthma, and also are the most prevalent diseases of the lower respiratory tract in general and most lethal after exclusion of cancer and infections in lungs [26]. Asthma is a heterogeneous disease, usually characterised by chronic airway inflammation [15]. COPD is a common preventable and treatable disease, characterised by persistent airflow limitation that is usually progressive and associated with enhanced chronic inflammatory responses in the airways and the lungs to noxious particles or gases [27]. Asthmatics especially are susceptible to COPD and smoking can result in a rapid loss of lung function in asthmatics [28]. Asthma and COPD may overlap in symptoms and occurrence in which case they are called ACOS (Asthma-COPD Overlap Syndrome) [29]. There is observed to be a significant increase in a number of senescent cells in the old lung and the diseased lungs of patients with COPD, Asthma or lung fibrosis [30] and this is illustrated in table 1.

Table 1: Respiratory disease incidence rates in elderly [31] [27]

	Old (45-54 years)		Senile	
	Incidence	% Deaths	Incidence	% Deaths
Chronic lower respiratory diseases	8.5	1.98%	638.2(85+)	4.27(85+)
Asthma	533	1.2%	699(85+)	11.6(85+)
COPD	6580	0.8%	11,557(75+)	0.45(75+)

Incidence is disease occurrence rates per 100,000 people from the USA. The percentage of death refers to the amount of deaths attributed to or linked COPD among the total percentage of deaths recorded in the given period. Though the percentage of deaths go down, the total no of deaths go up. This is rather due to the manifestation of other diseases of old age rather than decrease in effects of COPD pathology.

1.5 Telomere structure, dysfunction and senescence

Telomeres are short sequences of tandem TTAGGG repeats at ends of chromosomes. They are a unique feature of eukaryotes and discovered and named by Hermann J. Muller [32] and Barbara McClintock [33] in the 1930s. They form an essential protein-DNA complex that acts as a protective structure and prevents the degradation and fusion of chromosomes. The repeats are rich in guanine residues and protrude as a single stranded (SS) overhang. The implication of the SS overhang is that the recessed 5′ end-containing strand replicated by the leading strand synthesis machinery cannot function as a template for the synthesis of the 3′ overhang [34]. Hence, without the action of special maintenance mechanisms and telomerase activity, linear chromosomes experience end-replication problems and progressively shorten during each cycle of DNA replication. Telomere length thus limits the replicative potential of many normal human somatic cells [10]. Telomeres are also thought to be particularly prone to oxidative damage due to the high concentration of guanine residues [3]. Oxidative stress has been shown to accelerate the shortening of telomeres in cultured cells in vitro [35], however, more recently it has been shown that oxidative damage can also lead to telomere damage irrespectively of telomere length and telomerase activity [5] [36]. However, telomeres are protected by a group of protein complexes called shelterin. These result in telomeres coiling upon themselves to form a distinct T-loop structure [37]. The telomeres and shelterin complex together thus form a structure called as telosome. In general, the telomere is considered dysfunctional when the shelterin protein complex cannot effectively form a closed loop structure and exposes its end, thus activating a DNA damage response which may lead to senescence or apoptosis [38].

1.6 Telomere dysfunction and senescence in lung diseases

Telomere dysfunction has indeed been observed to play a vital role in various age-related diseases, and its role in senescence has received a lot of interest recently [39]. Telomere dysfunction can occur both as a normal function of cell and organism ageing as well as under various pathological conditions [40]. Pathological conditions that result in telomere dysfunction can be either non-genetic (benzene, radiation, ROS) [41] or genetic (TERT/TERC mutations)[33] genes or a combination as well. In Asthma and COPD it is believed to be a combination of genetic and environmental factors and especially for COPD, there is a strong correlation between smoking and exposure to toxic pollutants. In patients with Asthma [42] as well as in COPD patients [43] shortening of telomeres in leukocytes was observed previously, however particularly in Asthma the role of telomere dysfunction specifically in lung tissue has not been investigated until now.

1.7 Usage of Telomere Associated Foci as a mean to quantify cellular senescence

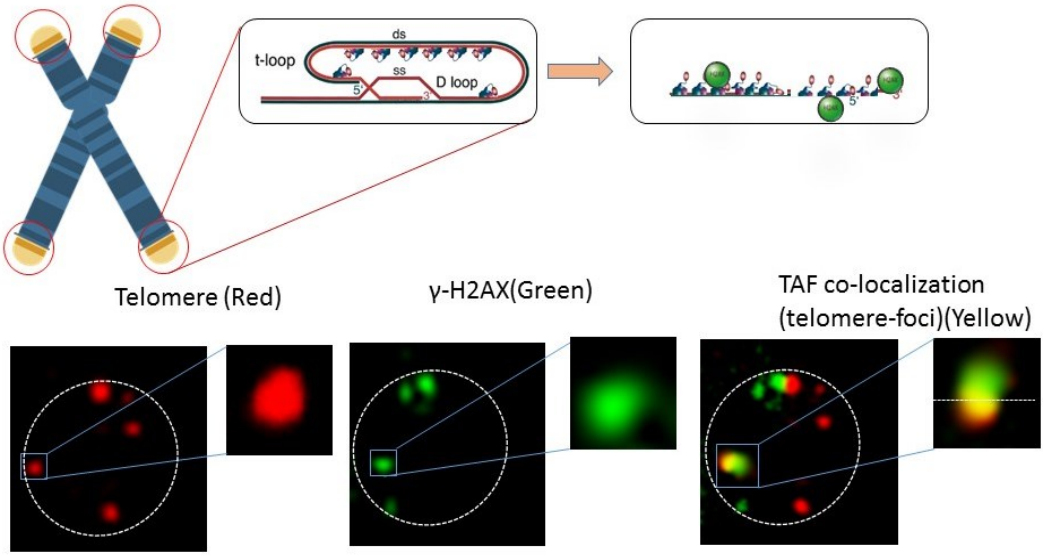

Figure 2: Telomere associated Foci. Telomeres stained by PNA probe appear red, DNA damage foci is visualized as green through hybridization with respective antibodies and region where DNA damage markers occur in conjunction with PNA probe appears yellow when a composite image is produced due to co-localization of both markers and this region is considered to be a region of damage in telomere or Telomere Associated Foci (TAF). TAF accumulates in senescent cells and are involved in induction of senescence as well, making them an ideal marker.

Since telomeres are primarily open strands of DNA that are capped by shelterin complexes. The disruption of the capping results in DDR activation and localization of response factors such as 53BP1, γ-H2AX, Rad17, ATM, and Mre11 [44] . Thus, even though there are no specific markers for telomere damage, co-localization of both telomeres and DDR factors can act as an indicator for damaged telomeres [5]. This telomere damage is visualised as regions of damage termed TAF (Telomere-associated foci) through Immuno-FISH by staining for both telomeres and Phosphorylated Histone 2.AX (γ -H2AX) a prominent marker for DNA Damage Response and quantification between the overlap of DNA damage response and telomere positions [45]. As mentioned previously, telomere damage irrespective of length can induce cellular senescence [5] . Thus, considering only telomere shortening as a factor driving senescence is a limited approach. By evaluating TAF, we can assess induction of damage at telomere irrespectively of their length- making it potentially a more reliable marker of telomere dysfunction than telomere length alone [36]. Hence, we studied *in vitro* mice models of asthma (mixed allergen) and COPD (smoke exposed), along with tissue biopsy sections from patient samples. Analysis of TAF will allow insight into the mechanisms underlying *in vivo* observations. Indeed previous studies have shown an association between reduced telomere length and damage in COPD in leukocytes [46] . In case of asthma reduced telomere lengths were observed in leukocytes [47], but there is no data on DNA damage and the data on leukocytes may not be reflective of lung condition [48].

1.8 Role of Mitochondrial Pyruvate carrier 1 in senescence

Recent studies have indicated mitochondrial dysfunction as an indicative factor for cellular senescence [49]. It is also indicated to be a significant element in the development of senescent phenotype [50] . MPC class of proteins is an evolutionarily conserved protein complexes essential for pyruvate transport [51] across all eukaryotes. In humans MPC1&2 are the primary carriers involved in pyruvate transport, they associate to form a 150 KDa complex on the inner membrane [52]. Previous data has also indicated that pyruvate might be a driving factor in senescence and the metabolic fate of it through the tricarboxylic acid cycle (TCA), and a possible determinant of induction of senescence [53]. Preliminary data from our lab has shown that MPC1is increased in human fibroblasts following induction of senescence. Moreover, data shows that the percentage of MPC1 positive cells increase with age in the small airways of ageing mice (Birch et al. unpublished). However, why MPC1 is increased and how this links to the mitochondrial dysfunction observed during cellular senescence [54] is not understood. Further studies will need to be conducted to evaluate the role of MPC1 during ageing lung and its effect on age-related lung diseases such as COPD.

Thus evidence suggests a strong link between cellular senescence and various lung diseases, it especially is well characterised regarding COPD [47] , though there are few studies that show reduced leukocyte telomere lengths [55] and indications of cytokine-induced senescence[56], data is still comparatively limited for asthma. The fact that these diseases are age linked and are aggravated by it alone are clear indicators of a probable link between them and further research into the underlying mechanisms of both diseases can reveal important new insights.

Aims

1. To determine whether telomere-associated foci show severity-dependent changes in chronic lung diseases.

2. To investigate telomere dysfunction and senescence in an allergen-exposed murine model and in lung tissue from asthma patients.

3. To determine whether MPC1 shows promise as a new senescence marker in lung disease.

Materials and Methods

2.1 Buffers and solutions

The solutions and buffers utilised are listed in Table 2

Table 2: Buffers and solutions

Reagent	Details
Histoclear	Clearing agent, Xylene substitute composed of ultra-refined light paraffin oil and orange oil by Fisher Inc, USA
Citrate buffer (0.01M)	29.41g of trisodium citrate, 1L of distilled H2O (pH 6.0)
Blocking reagent for immunofluorescence	Normal goat serum (NGS) in 0.1% BSA, diluted 1:60 to block nonspecific binding
PBS	Phosphate-buffer saline buffer solution (pH 7.4).
Primary & Secondary Antibodies(refer table 3.2)	
Avidin DCS	Fluorescein by Vector laboratories used to increase brightness of biotinylated secondary antibodies
Paraformaldehyde (4%)	Tissue section fixative
Maleic Acid	2.90175g maleic acid 250ml deionized water
Blocking Reagent for IHC and Immunofluorescence, Immuno-FISH	2 ml of 10× blocking reagent (Roche) 18ml maleic acid
Formamide	Organic solvent used for hybridization
Magnesium chloride buffer (MgCl2)	25mM magnesium chloride – 0.119g/50 ml dH2O

(pH 7.0)	9mM citric acid – 86.445mg/50 ml dH2O 82mM sodium hydrogen phosphate – 0.582g/50 ml dH2O (once made up, make 1 ml aliquot of MgCl2 buffer and store at -20°C)
Hybridization mix for Immuno-FISH	2.5ml 1M Tris buffer, pH 7.2 (1mM) 21.4ml MgCl2 buffer(pH7.0) 175ml deionised formamide 5ml of diluted PNA probe(1:10) (25mg/ml Applied Biosystems) 12.5ml of 1× blocking reagent (Roche) 33.6ml deionised water
Hydrogen Peroxide	Endogenous peroxidase activity blocker
Haematoxylin	5g Haematoxylin (Sigma, H3136), 300 ml Glycerin (Sigma, G2289), 50g Aluminium potassium sulphate (Sigma, 7210), 0.5g Sodium iodate (Sigma, S4007), 40 ml glacial acetic acid (Sigma, 537020) in 700 ml H2O
ProLong® Gold Antifade Mountant with DAPI	Used to mount tissue and provide a counterstain of blue (DAPI) for cells.

Table 3.A Primary antibodies used for immunofluorescence

Antibody	Species/Isotype	Specificity	Dilution	Product name/code
Anti-phospho-histone H2A.X (γH2A.X)	Rabbit	Mouse Human	1:250	9718-Cell Signalling
Anti-CD68	Mouse	Mouse	1:200	137001-Bio legend
Anti-Ki67	Mouse	Mouse	1:200	16A8-Bio legend
Anti- Mitochondrial pyruvate carrier 1	Rabbit	Mouse Human	1:200	14462 - Cell Signalling

Table 3.B Secondary antibodies used for immunofluorescence

Antibody	Species/Isotype	Specificity	Dilution	Product name/code
Anti-rabbit IgG Biotinylated	Goat	Mouse Human	1:250	VECTASTAIN Elite ABC Kit
Anti-rabbit IgG	Goat	Mouse Human	1:1000	AlexaFluor anti-rabbit 594
M.O.M biotinylated Anti-Mouse IgG	Mouse	Mouse	1:1000	BMK-2202, Vector labs

Table 3.C Primary antibodies used for immunohistochemistry

Antibody	Species/Isotype	Specificity	Dilution	Product name/code
Anti- Mitochondrial pyruvate carrier 1	Rabbit	Mouse Human	1:200	14462 - Cell Signalling

Table 3.D Secondary antibodies used for immunohistochemistry

Antibody	Species/Isotype	Specificity	Dilution	Product name/code
Anti-Rabbit IgG Biotinylated (VECTASTAIN Elite ABC Kit)	Rabbit	Goat	1:200	PK-6101-Vector Laboratories

2.3 Samples

2.3.1 Mice

A) Mice Mixed Allergen Model

All work was compiled with the guiding principles for the care and use of laboratory animals. All experiments were performed on lung tissues biopsy sections of four groups of mice. The respective groups included in whole two control groups and two mixed allergens (asthma phenotype). The asthma phenotype was induced by exposing the mixed allergen mice to a daily intranasal mixture of 10 mg of OVA and extracts from Alternaria, Aspergillus, and Dermatophagoides (house dust mite) for 4 weeks (Greer Labs), each dose in 50 ml of phosphate-buffered saline (PBS). The first control group had three mice each around 5-6 weeks old, and the second control group had 5 mice 18-21-month-old mice. In a similar manner, the mixed allergen mice had three mice of 5-6 weeks old, and other 5 had 18-21-month-old mice [57].

Table 4.1			
Mice	Age (months)	Allergen exposure duration (weeks)	No of samples
Mixed allergen (Young)	3-4	4	3
Control (Young)	3-4	-	3
Mixed allergen exposed(old)	6-24	4	8
Control(old)	6-24	-	8

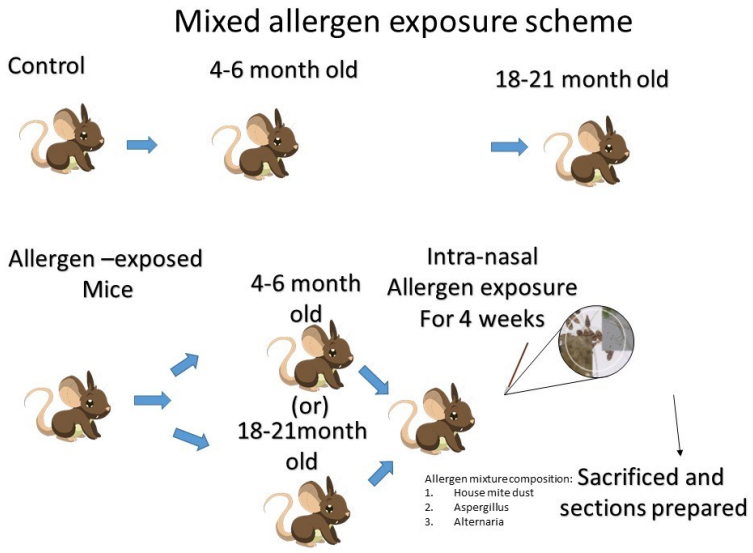

Figure 3.1: Scheme of mixed allergen exposure in mice

B) Mice Smoke-exposed model

All work was compiled with the guiding principles for the care and use of laboratory animals. At the start of the experiment, the animals were ten weeks old among which 12 controls were used, and 11mice were exposed to cigarette smoke for an hour twice for two weeks. After 24 hours of their last exposure to smoke, 6 of the controls and 6 of the smoke exposed mice were sacrificed, and tissue sections were made. After a recovery period of 7 days from exposure to smoke other six smoke exposed mice and five control mice were sacrificed and lung sections were prepared [58].

Table 4.2			
Mice	Age (months)	Smoke exposure duration(weeks)	No of samples
Mixed allergen (Young)	3-4	2 weeks (1x2 hr/day)	3
Control (Young)	3-4	-	3
Mixed allergen exposed(old)	6-24	2 weeks (1x2 hr/day)	10
Control(old)	6-24	-	10

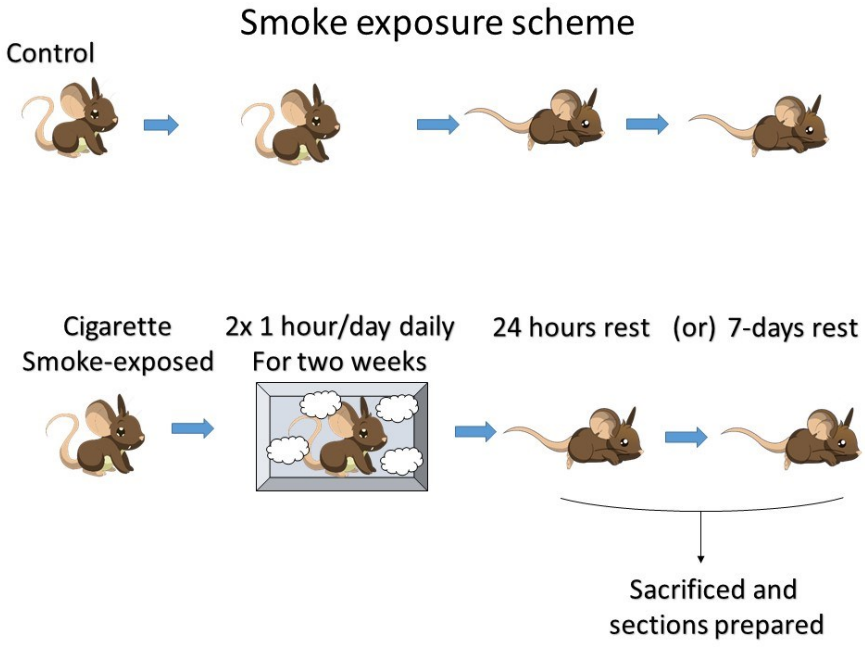

Figure 3.2: scheme of smoke exposure in mice

2.3.2 Humans

A) Lung biopsies- COPD

All human tissue samples were handled in accordance with rules of Human Tissue Authority, UK.

Paraffinized Human lung tissue from ten healthy volunteers and ten patients with moderate disease severity of COPD and ten severe disease condition of COPD obtained from MayoClinic, USA was used for experiments.

B) Lung biopsies- Asthma

All human tissue samples were handled in accordance with rules of Human Tissue Authority, UK.

Paraffinized Human lung tissue from two healthy volunteers and four patients with Asthma obtained from MayoClinic, USA was used to perform the experiments.

2.4 Deparaffinisation and rehydration of tissue sections

In order to prevent the loss of morphology and antigenicity of target molecules due during prolonged storage, Histological tissue sections are in general preserved using paraffin. Thus usage of stored sections for various experiments requires deparaffinisation. It is essential to deparaffinised the tissue sections to enable the reagents to access the cell/tissue components. To dewax the slides they were subject to a treatment of Histoclear (2x5 minutes), and they were then rehydrated by washing through graded ethanol (100%, 100%, 90%, 70%) for five minutes and then washed with tap water for another 10 minutes. The samples were then placed in Citrate buffer (0.01M, Ph 6.0) and microwaved for 5 minutes at high power (800w) followed by medium power (400w) for another 5 minutes and were allowed to cool down for (20-30 minutes) to retrieve the antigens. Samples were washed with distilled water (2x5 minutes) and used for further experimentation.

2.5 Immuno-fluorescence

The visualisation of target molecule/cell is through utilisation of fluorescent probes, which is done through the following method.

1. The deparaffinized sections were incubated in blocking reagents for 30 minutes at room temperature.
2. Tip-off the excess blocking buffer and incubate sections in diluted primary antibody overnight at 4*C.
3. Wash sections in PBS 3x5 minutes

2.5.1 Immunofluorescence in situ Hybridization for (Immuno-FISH) for detection of Telomere Associated Foci

The immunofluorescence carried out as per 2.5 was followed by FISH detection of DNA damage foci. Then the samples were incubated in biotinylated secondary antibody (goat anti-rabbit) for 30min at room temperature. After another set of PBS washes, samples were incubated with Avidin-DCS for 30 minutes and followed by PBS washes. The samples were then cross-linked by incubating in 4% PFA (Paraformaldehyde). After another set of PBS washes, they were dehydrated in graded ethanol solutions of (70%,90%,100%) for 3 minutes each and allowed to air dry briefly. The samples were then incubated with hybridization buffer containing telomere-specific PNA probe (Table 2) for 10 minutes Samples were then dried for 10 minutes in an oven and incubated in dark for 2 hours. The samples were then washed with PBS 3x5 times and washed in 70% formamide/2x SSC for 10 minutes. Then washed in 2x SSC for 10 minutes, followed by 3x10 minute wash in PBS. The samples were mounted with ProLong® Gold Antifade Mountant with DAPI as per 2.7

2.5.2 Staining for CD68

The first part of the experiment was carried out as mentioned in 2.4. Then the samples were processed with M.O.M kit (mice on mice) by Vector Labs (BMK-2202) as per the instruction of the manufacturer to eliminate unspecific binding and cross-reactivity of the secondary antibody.

2.5.3 Staining for MPC1

The experiment was carried out as mentioned in 2.4. Then the samples were incubated in secondary antibody for 30min at room temperature and mounted as per 2.7.

2.6 Immunohistochemistry

The samples were deparaffinized and rehydrated as mentioned in 2.4. Then the endogenous peroxidase activity was blocked by immersing sections in 0.9% H2O2 (Sigma, H1009) in distilled H2O for 30 minutes. Sections were then placed in running tap water and washed for 10 minutes, followed by a 5-minute wash in PBS. The incubation for blocking reagent and primary antibody were carried out same as mentioned in 3.4. The Incubation for secondary antibody was carried out as described in 2.5.4. Then 3x 5 min washes in PBS were followed with detection for secondary antibodies with rabbit peroxidase ABC kit (Vector Lab, PK-4001) as manufacturer's instruction. The substrates were developed with NovaRed kit (Vector Lab, SK-4800) according to manufacturer's instructions. The sections were then washed in tap water (3 x 1 minutes) before counterstaining nuclei with haematoxylin. Sections were dehydrated in graded ethanol solutions: 70%, 90%, 100% (1 minutes each) and cleared in histoclear (5 minutes) and mounted as per 3.6.

2.7 Mounting of stained tissue sections

The samples were washed 3x10 minutes in PBS and were mounted with ProLong® Gold Antifade Mountant with DAPI.

2.8 Microscopy

The stained slides were imaged by Broad-band fluorescence that was acquired from sections using X100 objective (TAF) & x64 Objectives (Macrophages & MPC1) respectively on Leica DMI8 inverted microscope. Sections were excited and fluorescence emission captured with Hamamatsu C11440-22 camera. For TAF the images were captured in 3 channels which were marked with respective colour by the imaging software the telomere as red, DNA-Damage foci gamma h2Ax as green and background DAPI (cell counterstain) in blue. The MPC1, CD68, Ki67, P21were imaged as two channel images with CD68 positive cells stained green against DAPI (cell counterstain) in blue and the same for MPC1 stained red. No notable differences among cells were found for Ki67 and P21 staining and thus were not further imaged as they could not be quantified. For samples stained through IHC for MPC1, Z-channels were not employed. Instead, they were imaged using a light microscope setting of Leica DMI8. The frequencies of excitation and resultant emission are listed below. All images in mice were obtained by imaging either small or large alveolar spaces of the tissue. In humans lung epithelial and parenchymal tissues were imaged as the airway structure was often highly degraded and thus could not be discerned and identified by visual observation.

Table 5	Rhodamine(Red)	GFP(Green)	DAPI(Blue)
Excitation Frequency	541-551 nm	450-490 nm	325-375 nm
Emission Frequency	565-605 nm	435-485 nm	500-550 nm

2.9 Quantification of images

The images were quantified using the software ImageJ by National Institute of health, Bethesda, Maryland, USA. A threshold was applied to images for optimum brightness and contrast. The values were then kept consistent for all images in a cohort that were quantified. All images were quantified in a blinded fashion.

2.9.1 TAF (Telomere Associated Foci)

TAF's were quantified using co-localization analysis, telomeres were rendered as red dots, while the gamma-h2x foci were seen as green. Movement through z-stacks revealed the location of gamma-h2x foci which were noted as points of DNA damage and at regions where the DNA damage Foci and Telomere overlapped were identified and marked as a region of damage in telomere. The number of telomere-associated Foci and number of DNA damage foci were recorded in 100 cells per sample and an average calculated.

2.9.2 Telomere Length

A boundary line was drawn around each cell and intensity of red dots were measured and mean value per cell was calculated by ImageJ, which was used as an indication of mean telomere length in a cell. Such values were calculated for 100 cells per sample, and the resultant value was averaged.

2.9.3 CD68 staining

Cells considered CD68 expression based on the appearance of staining were counted as macrophages and was divided by no of cells that do not show this characteristic and was converted into a percentage to obtain a relative rate of macrophage infiltration in the samples.

2.9.4 MPC1 (Mitochondrial Pyruvate Carrier 1)

The cells considered to have the MPC1 expression (brown colour in IHC/ red colour in IF) were counted and was divided by no of cells that do not show this characteristic and was converted into a percentage to obtain a relative rate of expression in the samples. The blue colour of nucleus from DAPI stain was used to discern the positively stained cells from the background.

2.10 Statistical analysis and graph generation

Mann-Whitney U test (one-tailed) was used to analyse the statistical difference between two groups. (Note: Mann-Whitney U test was because the data was not normally distributed and One-tailed as it was a measure of difference rather than increase). Spearman's rank was used to derive a coefficient of correlation and observe trend patterns. (Note: Spearman's rank was used as the data is non-parametric). Calculated Probability (P-value) below 0.05 were considered significant. All data analysis was carried out using Prism version 6.0, GraphPad Software, San Diego California USA and Microsoft Excel, Microsoft Corporation, Redmond, Washington, United States.

Results

3.1 Smoke exposed mice model

3.1.1 TAF and γ-h2AX levels were not changes in smoke exposed mice

Investigation of the involvement of DDR, telomere length and the presence of telomere associated foci were carried out by conducting immuno-FISH staining on mice lung sections from small airway regions (epithelial cells) as mentioned in methods previously. Increase in DNA damage is seen 24 hours after the last smoke exposure and appear to remain persistent. There was no significant change in mean no of TAF nor percentage of cells with TAF, though a tendency of increase post smoke exposure is observed. There were no significant changes in mean telomere lengths.

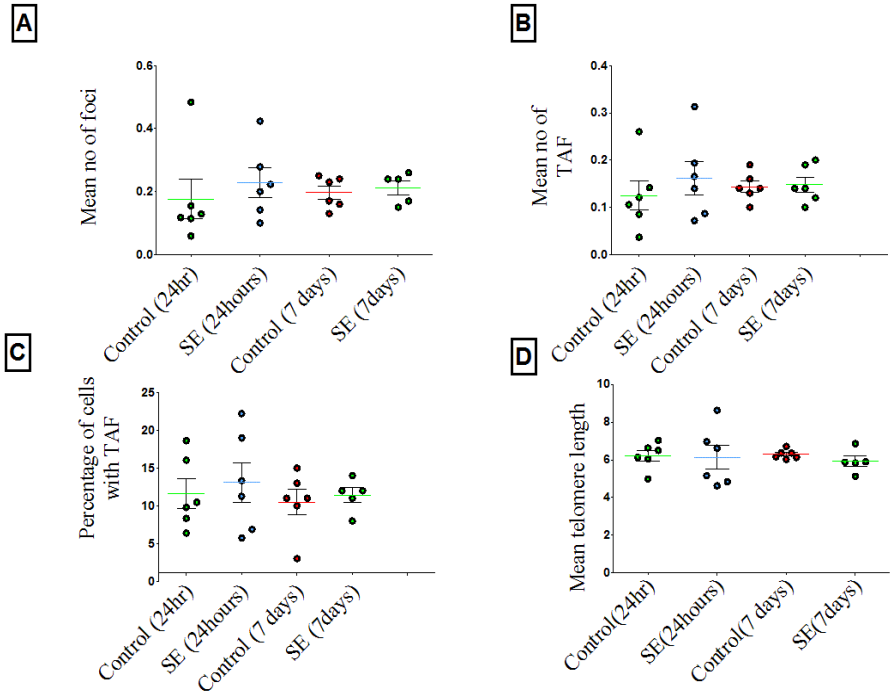

Figure 4.1: Analysis on DNA damage foci with phosphorylated H2A.X (γ-H2AX), telomere-associated foci (TAF) and telomere length in small airway epithelial cells of wild type and Smoke exposed mice for time points 24 hours and 7 days. Small airway epithelial cells from wild type and smoke exposed mice were stained forγH2A.X and telomeres by immuno-FISH. Dot plots represent mean number of γH2A.X (A),mean number of TAF (B), percentage of cells containing TAF (C) and mean telomere length (D)for each mice, obtained by quantifying Z-stacks of minimum 100 cells per subject. Telomere length was generated using ImageJ by measuring its intensity on red channel. Data are presented as the mean for individual subjects. Blinded fashion quantification method was carried out in this experiment. Horizontal lines represent group median. (TAF). Statistics: Mann-Whitney U test. *p < 0.05, 24 hour TAF data provided by J Birch

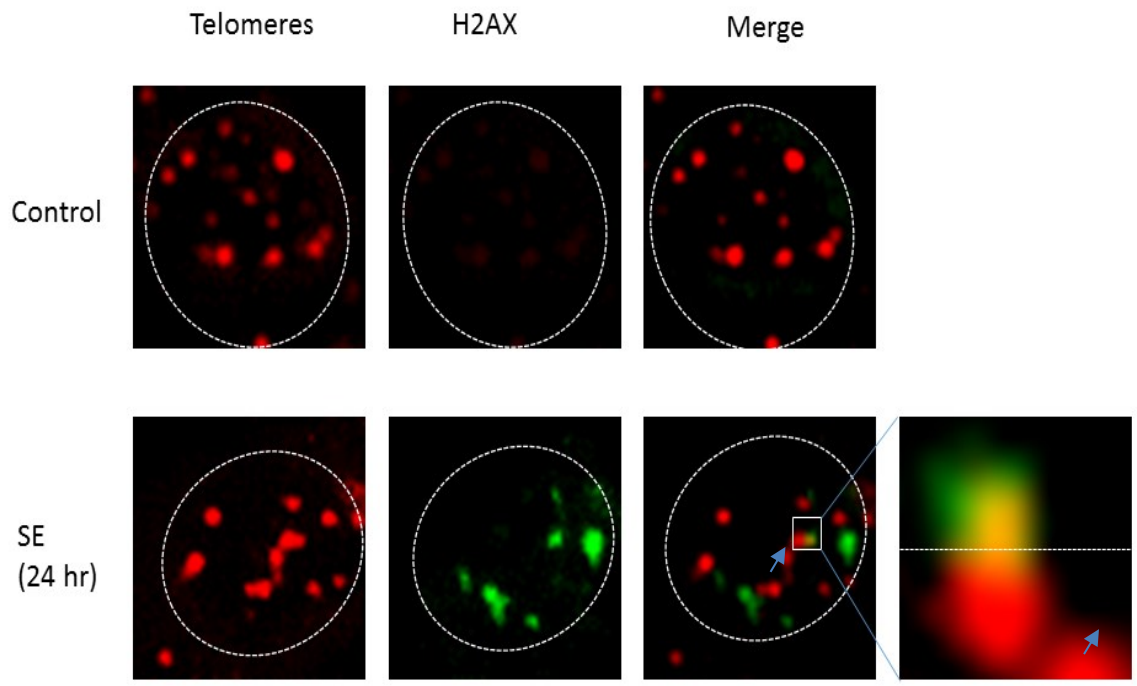

Figure 4.2 : Representative image of immuno-FISH staining for γH2A.X (green) and telomeres (red) in small airway epithelial cell, wild-type, smoke exposed mice after 7 days. Images were taken under X63 oil objective. Arrow points to co-localisation ofγH2A.X and telomeres.

3.1.2 Smoke exposed mice do not show increased expression of MPC1

Investigation of the involvement of MPC1 were carried out by conducting immunohistochemistry staining on mice lung sections from small airway regions (epithelial cells) as mentioned in methods previously. A small tendency for an increase in MPC1 levels is seen 24 hours after the last smoke exposure, however, it is not statistically significant.

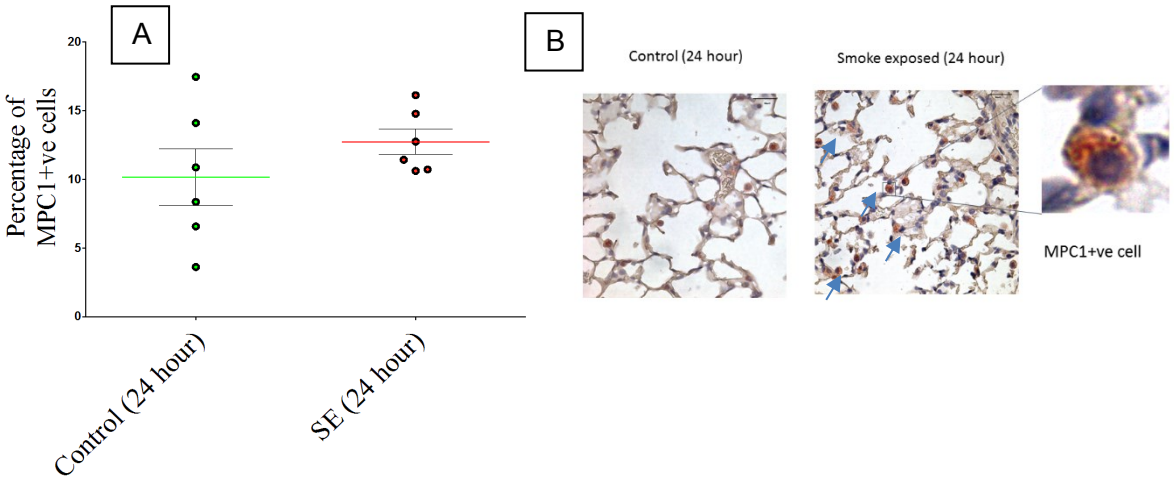

Figure 4.3: (A) Data represents relative levels of MPC1 expression in lung tissue section (small airway) of wild-type and smoke exposed mice (24 hour cohort). Identification of MPC1+ve cells was carried out using immunohistochemistry staining on small airway lung tissue sections, in order to quantitatively work out the total number of positive cells per images. Blinded fashion quantification method was carried out in this experiment. Dot plot represent the mean number of MPC1+ve positive cells per field for each animal, with horizontal line representing group median. **(B) Representative images for MPC1+ve wild-type, Smoke exposed mice**, taken under X40 objective. Arrows point to MPC1 positive cells. Statistics: Mann-Whitney U test. * $p < 0.05$

3.1.3 MPC1 and TAF levels do not show any significant correlation

The data previously obtained about TAF and MPC1 were analysed using Prism 5 to see if there were any patterns of correlation between no of TAF and MPC1 levels. Pearson's test was utilized for this. R represents the correlation co-efficient and P the significance ratio. No statistically significant patterns of correlation were observed.

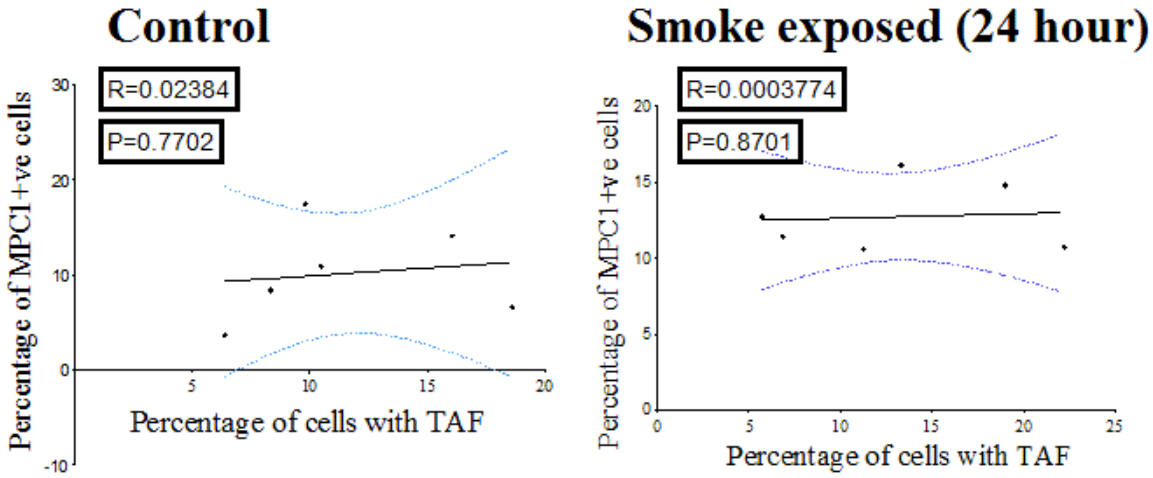

Figure 4.4: Correlation Analysis Telomere 2A.X (γ-H2AX), telomere-associated foci (TAF). Each box plot represents mean value of sample mentioned in Graphs A & B. The mean value of MPC1% is plotted against Y axis, while mean Value of TAF% is plotted in X axis and a trend line is drawn through. Statistical analysis was performed using Pearson's correlation. Left the respective values from the control sample, Right represents the values from smoke exposed mice. Statistics: Pearson's rank correlation

3.2 Mixed allergen exposed mice model

3.2.1 TAF and γ-h2AX levels showed a reduction in mixed allergen exposed mice

Investigation of the involvement of DDR, telomere length and the presence of telomere associated foci were carried out by conducting immuno-FISH staining on mice lung sections from large airways and small airway regions (epithelial cells) as mentioned in methods previously. Increase in DNA damage foci, mean no of TAF and percentage of cells with TAF was observed to increase over age. Mixed allergen group showed reduced levels of DNA damage foci, mean no of TAF and percentage of cells with TAF compared to wildtype controls. The observed pattern was statistically significant in old cohort of control vs mixed allergen, trend was still visible in the young but was not statistically significant. There were no significant changes in mean telomere lengths in both cohorts.

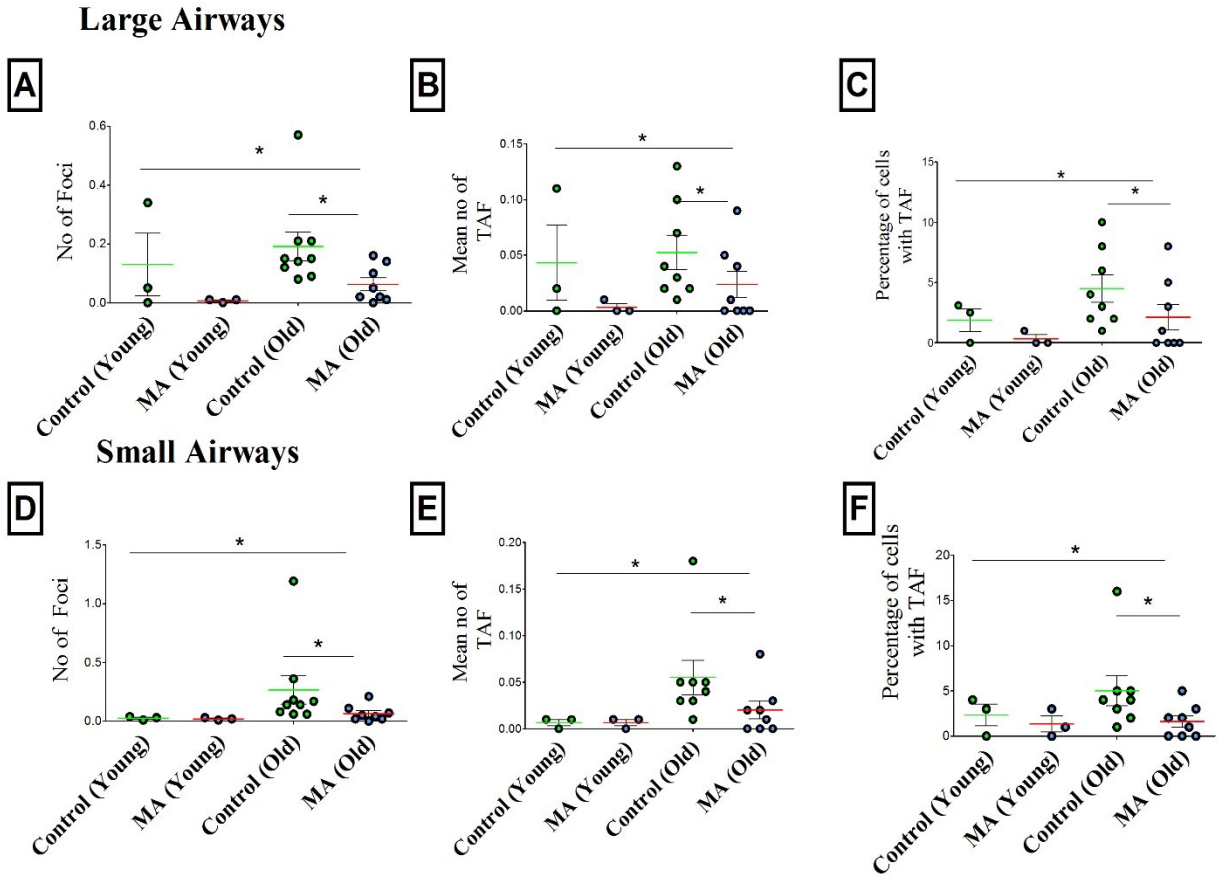

Figure 5.1: Analysis on DNA damage foci with phosphorylated H2A.X (γH2AX), telomere-associated foci (TAF) and telomere length in airway epithelial cells of wild type and mixed allergen exposed mice for time points 3-4 months old and 6-24 months old. Small airway epithelial cells from wild type and mixed allergen exposed mice were stained forγH2A.X and telomeres by immuno-FISH. Dot plots represent mean number of γH2A.X (A) for large airways and (D) for small airways, mean number of TAF (B) for large airways and (E) for small airways, percentage of cells containing TAF (C) for large airways and (F) for small airways and mean telomere length (G) for each mice, obtained by quantifying Z-stacks of minimum 100 cells per subject. Statistics: Mann-Whitney U test. *p < 0.05

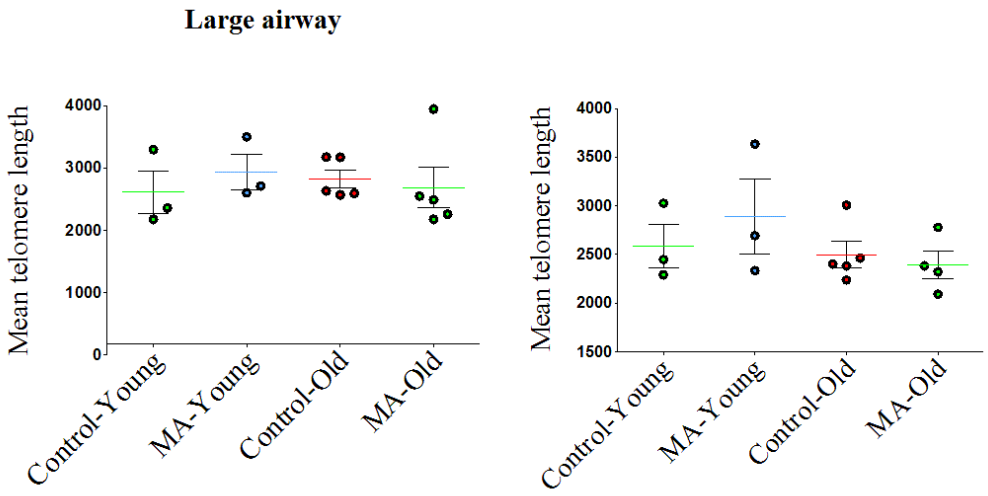

Figure 5.2 Telomere length was generated using ImageJ by measuring its intensity on red channel. Data are presented as the mean for individual subjects. Horizontal lines represent group median. Statistics: Mann-Whitney U test. * p < 0.05

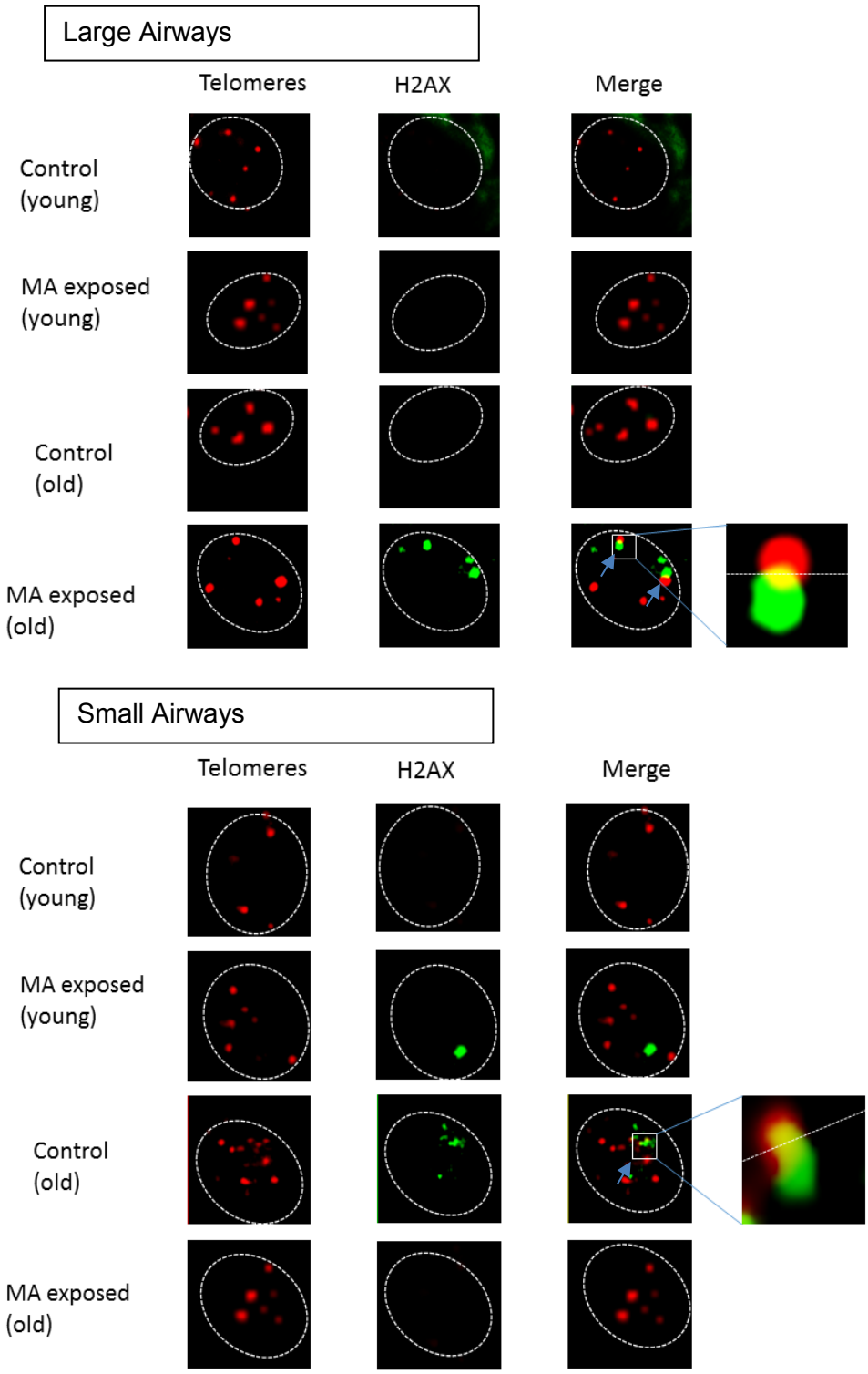

Figure 5.3: Representative image of immuno-FISH staining for γH2A.X (green) and telomeres (red) in small airway epithelial cell, (from top left to bottom right, in horizontal manner) wild-type, smoke exposed mice after 24 hours, wild-type, smoke exposed mice after 7 days. Images were taken under X63 oil objective. White arrow points to co-localisation ofγH2A.X and telomeres (TAF

3.2. Mixed allergen mice had higher levels of macrophages (CD68 marker)

Investigation of the involvement of macrophages as a possible clearance mechanism of senescent cells were carried out by conducting immunohistochemistry on mice lung sections from small and large airway regions (epithelial cells) as mentioned in methods previously. Statistically significant increase in CD68 levels were seen in mixed allergen model when compared to controls in young cohort.

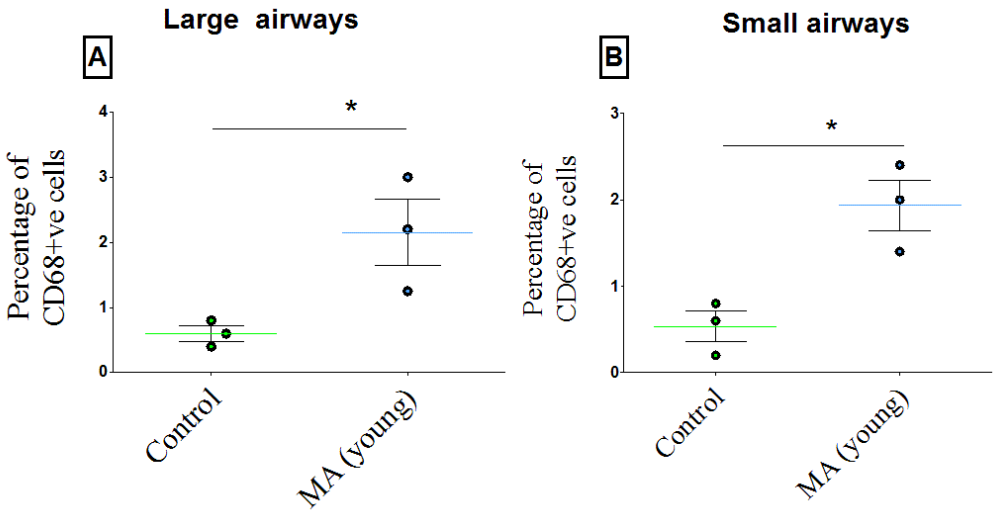

Figure 5.4: Data represents levels of macrophage infiltration in lung tissue of wild-type and MA allergen exposed mice. Identification of CD68+ cells was carried out using immunofluorescent staining on lung tissue sections, in order to quantitatively work out the total number of positive cells per images. Blinded fashion quantification method was carried out in this experiment. Dot plot represent the mean number of CD68 positive cells per field for each animal, with horizontal line representing group median. (A) Represents data from large away sections and (B) from small airway sections. Statistics: Mann-Whitney U test. * $p < 0.05$

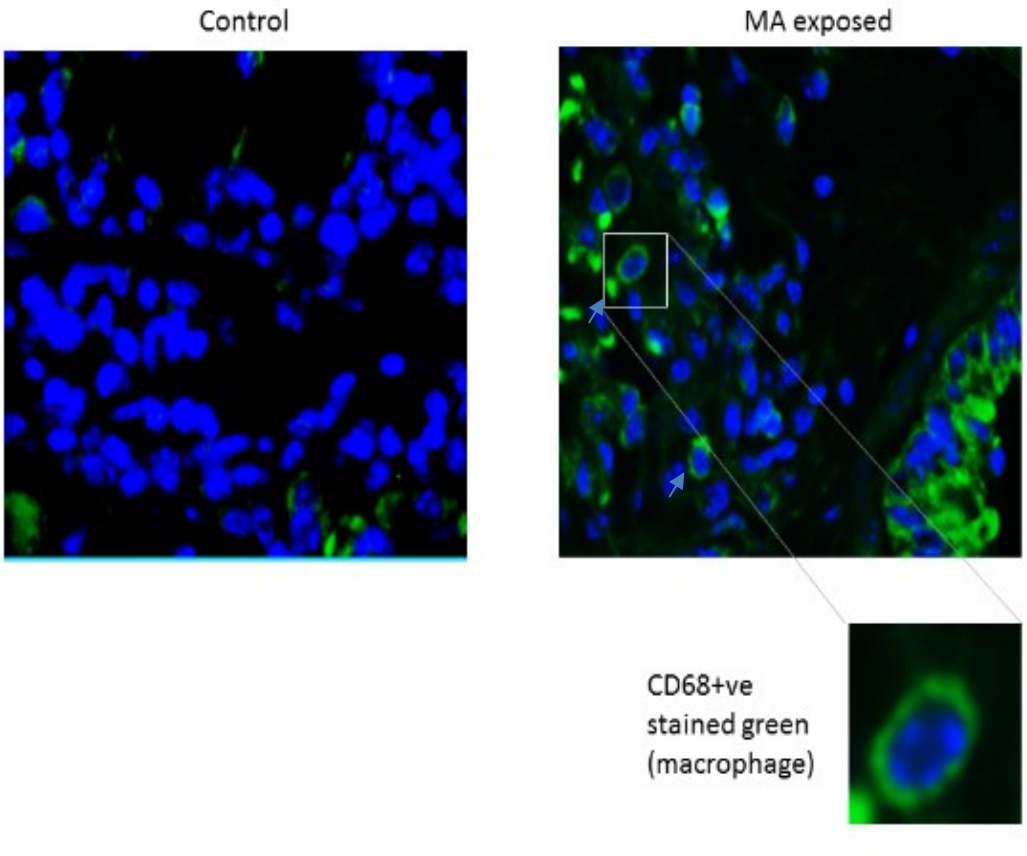

Figure 5.5: Representative images for macrophage infiltration (from top left to bottom right, in horizontal manner) wild-type, Mixed allergen exposed mice, taken under X40 objective. Arrows point on positive cells.

3.3 Human COPD patient biopsies

3.3.1 TAF and γ-h2AX levels increased with progression of disease condition

Investigation of the involvement of DDR, telomere length and the presence of telomere associated foci were carried out by conducting immuno-FISH staining on human lung sections from epithelial and parenchymal regions as mentioned in methods previously. Increase in mean no of DNA damage Foci and TAF was observed to show a statistically significant correlative increase along with increase in disease severity. There were no significant changes in mean telomere lengths and percentage of cells with TAF, however when analysed for no of cells with two TAF or more, statistically significant correlative increase along with disease severity similar to prior data was observed.

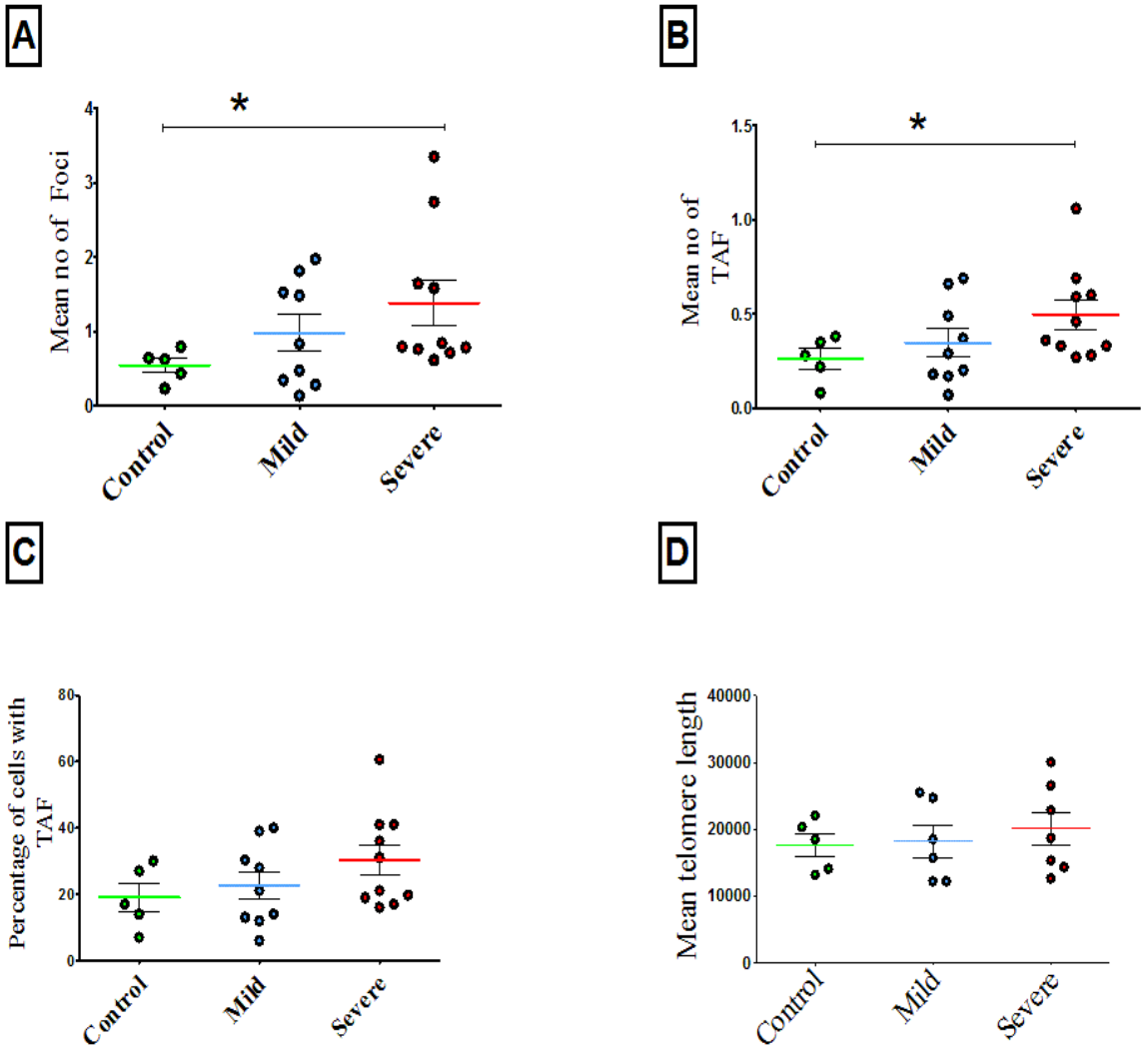

Figure 6.1: Analysis on DNA damage foci with phosphorylated H2A.X (γH2AX), telomere-associated foci (TAF) and telomere length in lung biopsy sections of healthy, moderate and severe patients of COPD. Biopsy sections from patients were stained forγH2A.X and telomeres by immuno-FISH. Dot plots represent mean number of γH2A.X (A) mean number of TAF (B) percentage of cells containing TAF (C) and mean telomere length (D) for each patient, obtained by quantifying Z-stacks of minimum 100 cells per subject. Telomere length was generated using ImageJ by measuring its intensity on red channel. Data are presented as the mean for individual subjects. Horizontal lines represent group median. Statistics: Mann-Whitney U test. *p < 0.05

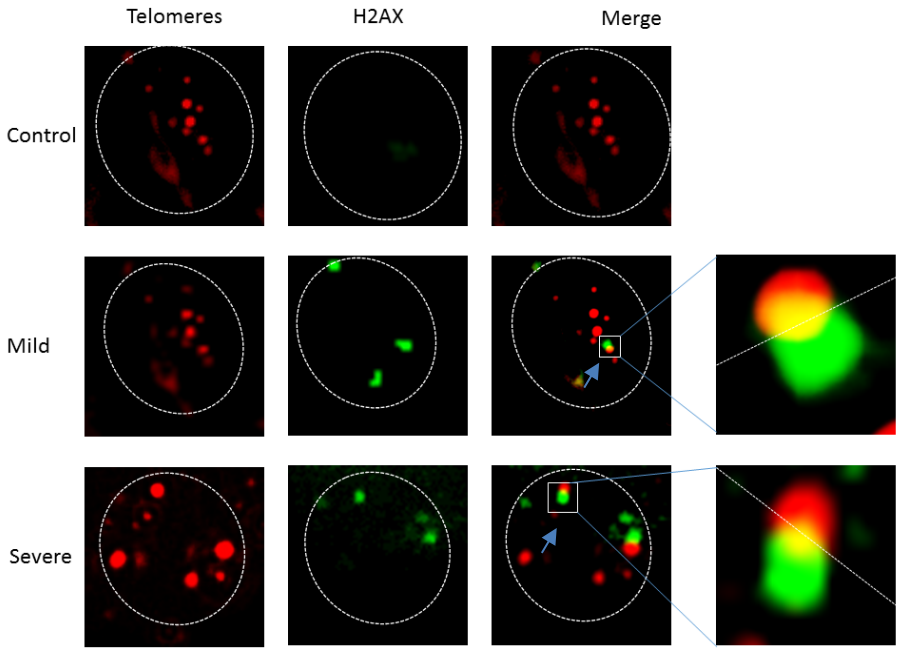

Figure 6.2: Representative image of immuno-FISH staining for γH2A.X (green) and telomeres (red) in small airway epithelial cell, (from top left to bottom right, in horizontal manner) wild-type, smoke exposed mice after 24 hours, wild-type, smoke exposed mice after 7 days. Images were taken under X63 oil objective. White arrow points to co-localisation ofγH2A.X and telomeres

3.3.2 MPC1 levels show increase along disease severity

Investigation of the involvement of MPC1 were carried out by conducting immune-FISH staining on human lung sections from parenchymal and airway sections (epithelial cells) as mentioned in methods previously. Increase in percentage of cells with MPC1+ve stains was observed to show a correlative increase along with increase in disease severity.

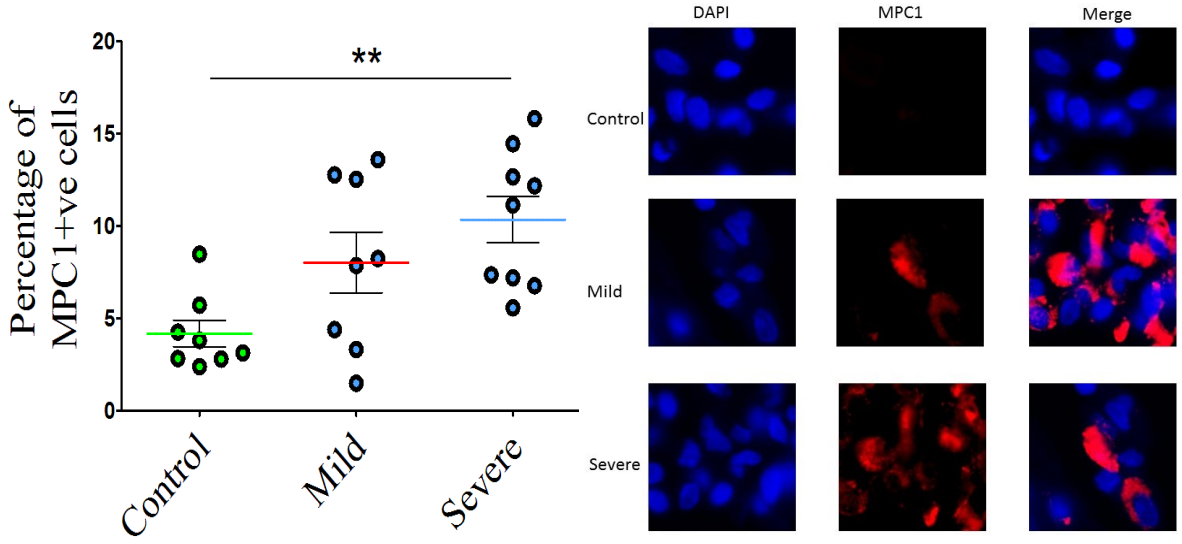

Figure 6.3: Data represents levels of MPC1 expression in lung tissue of healthy, Mild and Severe COPD patients. Identification of MPC1+ve cells was carried out using immunofluorescence staining on lung tissue sections, in order to quantitatively work out the total number of positive cells per images. Blinded fashion quantification method was carried out in this experiment. (A) Dot plot represent the mean number of MPC1+ve positive cells per field for each subject, with horizontal line representing group median. (B) Representative images for MPC1+ve wild-type, Human epithelial/parenchymal lung sections, taken under X63 objective. Negative cells (seen fully blue) and positive cells (seen with red stains). Statistics: Mann-Whitney U test. * $p < 0.05$

3.3.3 MPC1 and TAF levels do not show any positive correlation

The data previously obtained about TAF and MPC1 were analysed using Prism 5 to see if there were any patterns of correlation between TAF and MPC1 levels. Though both values show a similar patterns of correlative increase along with disease severity, they do not correlate with each other on analysis of individual samples.

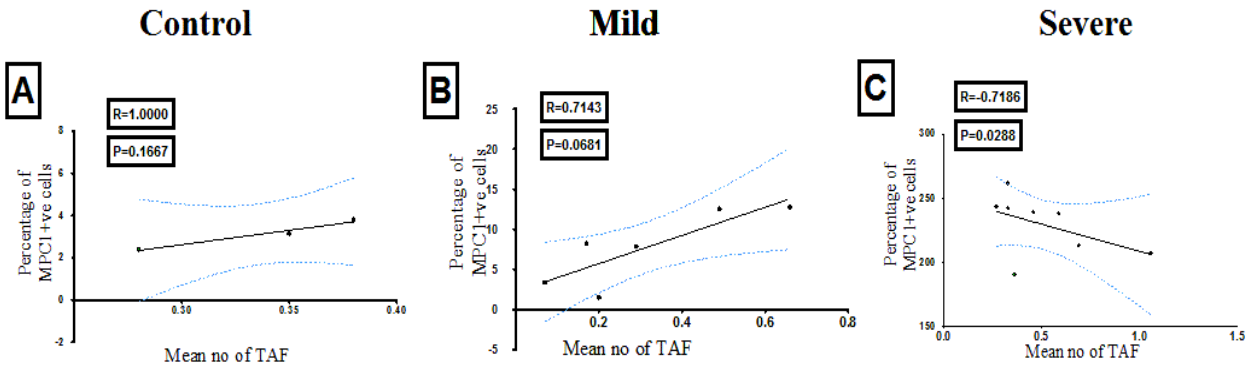

Figure 6.4: Correlation Analysis Telomere 2A.X (γH2AX), telomere-associated foci (TAF). Each box plot represents mean value of sample mentioned in Graphs 4.2.1 & 4.2.2. The mean value of MPC1% is plotted against Y axis, while mean Value of TAF% is plotted in X axis and a trend line is drawn through. Statistical analysis was performed using Pearson's correlation. (A) Represents the respective values from the control sample, while (B) represents the values from patients of moderate/mild COPD and (C) for severe Statistics: Pearson's rank correlation test

3.3.4 Fev-1- MPC1 and TAF levels do not show any correlation

The data previously obtained about TAF and MPC1 were analysed using Prism 5 to see if either one or both of their levels also correlated with increased/decreased lung function. The data revealed no distinct trends of correlation with lung function and was not statistically significant.

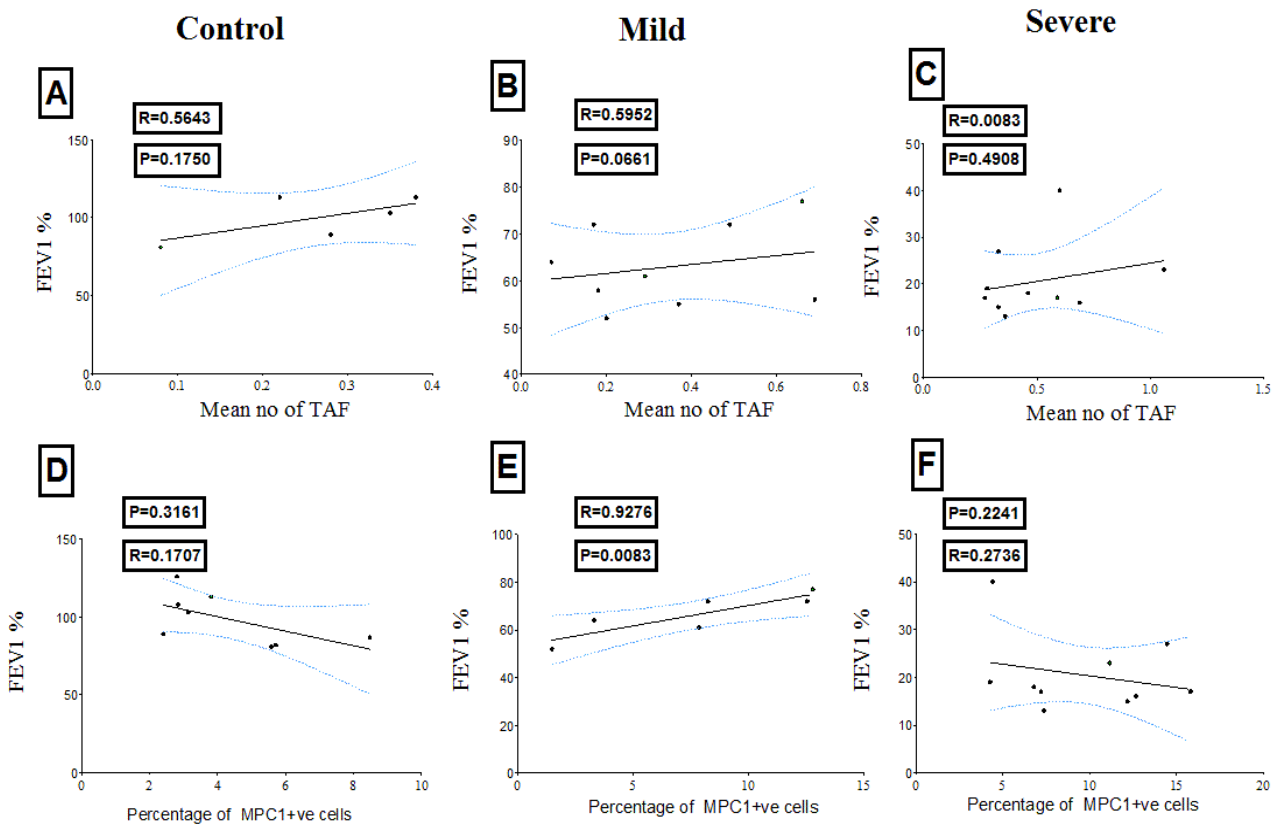

Figure 6.5: Correlation Analysis of telomere-associated foci (TAF) and MPC1 against FEv1 %(lung function value). Each box plot represents mean value of sample mentioned in Graphs 6.1 & 6.3. In the top row the mean value of TAF is plotted against Y axis, while mean Value of FEV1% is plotted in X axis and a trend line is drawn through. In bottom row mean value of MPC1% is plotted against Y axis, while mean Value of FEV1% is plotted in X axis and a trend line is drawn through .Statistical analysis was performed using Pearson's correlation. (A) (D) Represents the respective values from the control sample, while (B) and (e) represents the values from patients of moderate COPD and (C) for severe. Statistics: Pearson's rank correlation test

3.4 Human Asthma patient biopsies

3.4.1 Immuno-FISH in control and Asthma patients.

Investigation of the involvement of DDR, telomere length and the presence of telomere associated foci were carried out by conducting immuno-FISH staining on human lung sections from epithelial and parenchymal regions as mentioned in methods previously. There were not sufficient samples to perform statistical analysis, but a trend of increase along with disease severity was observed in mean no of DNA damage foci, mean no of TAF and percentage of cells with TAF. There were no significant changes in mean telomere length.

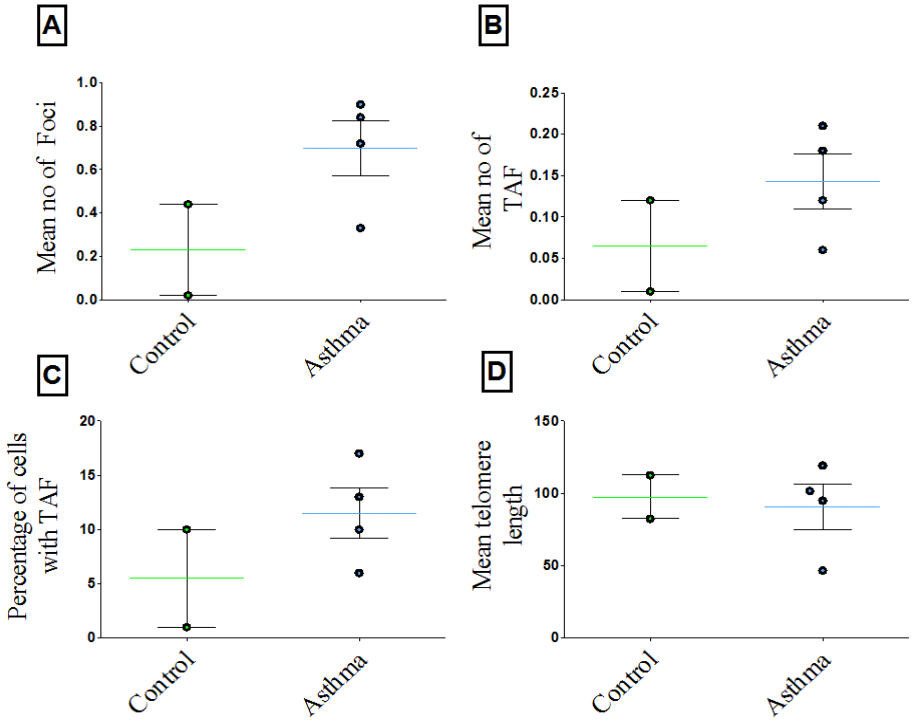

Figure 7.1: Analysis on DNA damage foci with phosphorylated H2A.X (γH2AX), telomere-associated foci (TAF) and telomere length in lung biopsy sections of healthy and asthma patients. Biopsy sections were stained forγH2A.X and telomeres by immuno-FISH. Dot plots represent mean number of γH2A.X (A) mean number of TAF (B) percentage of cells containing TAF (C) and mean telomere length (D) for each patient, obtained by quantifying Z-stacks of minimum 100 cells per subject. Telomere length was generated using ImageJ by measuring its intensity on red channel. Data are presented as the mean for individual subjects. Horizontal lines represent group median. Statistics: Mann-Whitney U test. *$p < 0.05$

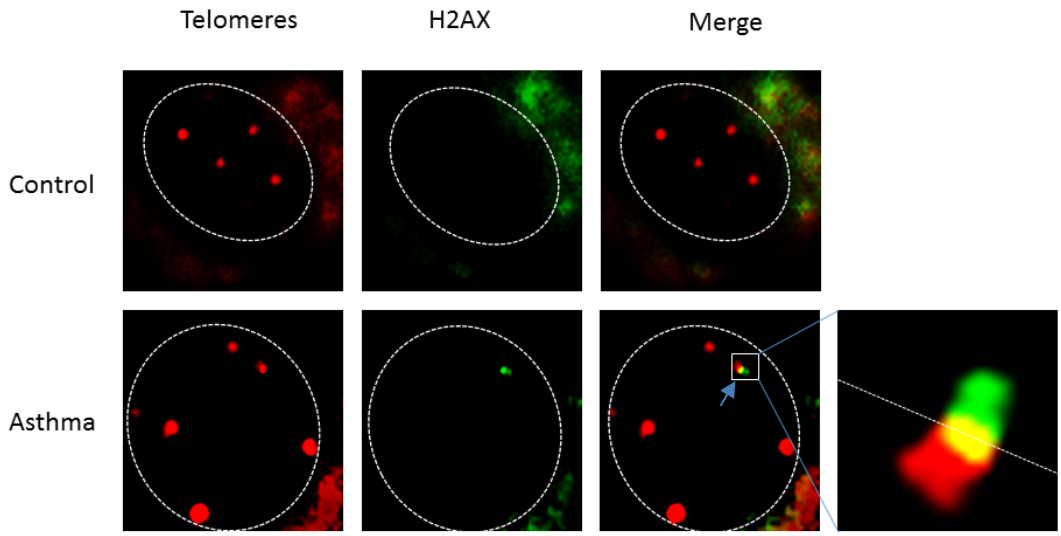

Figure 7.2 : Representative image of immuno-FISH staining for γH2A.X (green) and telomeres (red) in small airway epithelial cell, (from top left to bottom right, in horizontal manner) wild-type, smoke exposed mice after 24 hours, wild-type, smoke exposed mice after 7 days. Images were taken under X63 oil objective. arrow points to co-localisation ofγH2A.X and telomeres

Discussion

Age-related diseases of multiple organs have now been linked to cellular senescence and with lungs being the primary targets of ROS and other cytotoxic stresses from the environments. Assessment of cellular senescence in it would enable further insights into its diseases. However, as the majority of results and data is carried out in mice, validity of such data and it's translation into the human state has been rather questionable [59]. In this study, we performed analysis on both *in vivo* mice models of lung diseases as well as on human patient biopsies.

Our results indicate that under our experimental conditions there were no significant differences in telomere dysfunction or overall DNA damage in small airway epithelial cells immediately following cigarette smoke exposure or 7 days after. This is in contradiction with recent data which indicate that TAF can be induced by cigarette smoke [47]. Telomere length and MPC1 levels showed no statistical difference between all cohorts either. However, lack of changes in TAF or DNA damage levels does not necessarily mean cigarette smoke exposure is harmless in mice, as there indeed is a wealth of evidence indicating its effect on DNA and telomere damage [60] [61]. This might merely be due to the short duration of the smoke exposure period which though particularly not for TAF, still has been documented when checked for other age related lung disease parameters and pathways [61]. In one particular study mice showed recovery of health 8 weeks after smoke exposure, though they were given 8 weeks of rest as well [62], compared to two weeks of smoke exposure and a day/week rest in our project. None the less, there is an indication at least that mice are capable of recovery post smoke exposure. While, its ability to translate into a descriptor of human pathology is indeed difficult, a recent study of global lifespan among smokers indicated, that quitting smoking prior to age of 30 reduces risk of smoke related disease mortality levels to percentages similar to that of a non-smoker [63]. However, the results could be not due to lack of damage but due to the damage inducing apoptosis in lung epithelial cells. Previous studies have shown that cigarette smoke exposure can induce over expression of ApoA1 (apolipoprotein 1) which results in enhanced apoptosis in cells and extensive remodelling of lung tissue architecture [64]. This was seen to inhibit chronic lung inflammation and attenuation of the disease pathology. It would be ideal thus to utilize markers of lung inflammation such as C-protein, TNF-alfa, IL-6 or IL-8[65] along with TAF measurements in future studies to understand if it might be apoptotic remodelling or lack of DNA/telomere damage.

This might prove essential as our hypothesis primarily relied on an assumption of mice models being susceptible to same kind of damage as humans. However, this might not be always true as different strains seem to show a different pattern of inflammageing (inflammatory ageing) on exposure to cigarette smoke [66] and it is essential to identify whether the observed data is due to quirks of the particular strain or this is a standard response mechanism across the board.

Staining in parenchymal/epithelial lung sections of human patients of COPD, the number of TAF revealed a statistically significant increase with the development of COPD. Even moderate cases of COPD patients showed slightly albeit non-significant increase in TAF when compared to controls. Previous work had shown that severe COPD patients had increased TAF [47]. However this is the first time that TAF has been studied in tissues from moderate COPD patients. This data suggests that TAF is not merely the outcome of the disease but may be causal in the process. Consistent with a causal role for telomere dysfunction in lung disease- telomere dysfunction in late-generation TERC-/- mice has been shown to induce TAF and emphysema-like changes in lung [47]. MPC1 percentage levels displayed the same trend with statistically significant increase between control and severe groups and a non-significant increase in mild over the control. When correlation analysis was performed a non-significant trend of mutual increase between percentage of MPC1 positive cells as seen in figure 6.4 (A) (B) and TAF was observed in control and moderate samples. The trend showed a reversal in tissue samples of people with severe levels of COPD as indicated in figure 6.4 (C). One apparent hypothesis to explain this could be induction of Warburg effect that results in the cells becoming cancerous with the result being the repair of telomeres. However this assumption is challenged as MPC1 is indicated to be a repressor of Warburg effect [67]. In terms of TAF levels observed in our project, and in context of COPD, a particular study in 2014 by Stanley et al is of relevance [68]. His team observed that patients with certain TERT and TR mutations were more susceptible to occurrence of COPD and rare variants of TERT clustered with COPD phenotype. This particularly is relevant in context of our investigation as TERT mutations are also responsible for enhanced cellular senescence [2]. Thus it is possible that the respective TERT mutations might be responsible for both enhanced cellular senescence and COPD phenotype, rather than cellular senescence leading up to COPD phenotype. Since, the patients in this cohort were not genotyped, the hypothesis thereby remains untested.

Telomere lengths showed no statistically significant changes, which was in line with previous data from our lab [47]. However, in terms of hypothesis mentioned prior, if TERT mutations were involved it would shortening of telomeres as seen in cases of patients of Idiopathic Pulmonary Fibrosis [69].

Overall however data suggests that telomere dysfunction does indeed increase with age and might even be a driving factor for age-related diseases in lungs, but the mice models utilised for this purpose may not accurately represent the conditions of disease and occurrence of cellular senescence in humans. It also suggests that MPC1 a newly identified monomer of MPC1-MPC2 protein complex might be a marker for senescence and can be used as a biomarker of COPD since it correlates with disease progression. Though due to the limited scope of the project and relatively low no of samples, the data must be further evaluated for an effective conclusion. Hence, MPC1-MPC2 complex seems as an ideal candidate for further evaluation as a marker for senescence.

In mice that have been exposed to mixed allergens, there is reduced a number of DNA damage foci and telomere-associated foci in the allergen-exposed mice compared to control. It was hypothesised whether if this could be because of increased immune activity and inflammation that might be clearing out senescent cells more in the MA mice[70][71]. When tested for this hypothesis, the mice exposed to mixed allergen indeed were shown to have higher no of macrophages in the lung compared to the control group (refer figure). Macrophages have been previously involved in the clearance of senescent cells from tissues [70, 72, 73]. This held true for in both the young and old mice exposed to a mixed allergen, though when the comparison was done between young and old mice, in both MA and control group there was an increase along with the progression of age, which has been described previously [50]. The variation in telomere lengths however in both groups were not statistically significant though as a slight age-related decrease in length was observed. As mentioned prior for the smoke exposure experiments, measurements of inflammation markers would also be ideal for this study in future. Mixed allergen exposed mice models also show strain dependent variations [74] and thus would be ideal to be conducted on various strains to obtain data of high reliability.

In human patients with Asthma TAF and DNA damage foci are both increased. However, due to the small size of the sample, statistical analyses could not be carried out. For the same reason despite the observation of reduced telomere length, statistical significance could not be derived from it. However, these data were in line with previous data on leukocytes of asthmatics [10], as mentioned before. Nevertheless, leukocyte data are not reflective of the lung condition and lung section data from this study is too small to validate it.

Conclusion

From this study, we have found that asthma and COPD patient might be due to increased levels of telomere dysfunction. The mouse model, however, was not reflective of the severity observed in human models, indicating that they may not be robust enough to study human disease conditions in lungs. MPC1 promises to be an ideal candidate as a senescent marker.

Future work

Ideal targets for future work would include testing on larger sample sizes, as well as segregation of disease conditions based on age group as another variable. It would also be ideal to stain for markers of inflammation such as IL-6, IL-8, and TNF-alfa etc. to understand morphological organ-wide changes in disease pathology in conjunction to DNA/Telomere damage. Genotyping the patients for the occurrence of TERT/TR mutations would also be of interest. To ensure the models used for the studies are ideal. It would also be essential to conduct the experiments in different strains of mice along with various durations of smoke exposure and mixed allergen exposure with both treatment and measurement multiple time points and a longer duration/age range. MPC1 as a marker can only be confirmed if tested on for more diseases and the methods employed in the current study can be transferred for studies on other lung diseases such as bronchitis, pulmonary fibrosis and emphysema. Further work on MPC1 would also involve it to be tested in tangent with other senescence markers such as p21, p53 and such to observe its effectiveness on the said sample. Exploration of other techniques such as western blotting and RT-PCR is also of interest in the context of studying MPC1 expression levels. The purpose who whose would be to obtain enough data and construct a fully characterised model to understand etiological reasons of senescence in lungs.

Acknowledgements

I would like to thank Dr Joao Passos, for providing me with a chance to work in his lab. I would also like to thank Dr Jodie Birch and Anthony Lagnado for their continuous support and providing me assistance in the lab. In specifics Jodie for the provision of images of smoke-exposed mice, which were essential for my quantifications and Antony who helped me conduct numerous experiments and provided support and performed the IHC for MPC1 in mice without which I would not have been able to quantify and derive the data required. However, my thanks do not stop with mere acknowledgements for technical help, but also extends further as they supported me not just in lab work, but also by providing guidance on my future career, helping me resolve my concerns and anxiety on research and by being great mentors overall. However, it would be unfair to conclude by not acknowledging other lab members, Stella, James, Edward and Hanna, who helped me through various means as well. Finally, I would like to thank you to my parents, grandparents, friends and my dog, who encouraged me and provide moral support for me to study at the university. In words of Isaac Newton, I was only able to see further than others because I was able to stand on shoulders of giants.

References

1. Harley, C.B., A.B. Futcher, and C.W. Greider, *Telomeres shorten during ageing of human fibroblasts.* Nature, 1990. **345**(6274): p. 458-460.
2. Campisi, J. and F. d'Adda di Fagagna, *Cellular senescence: when bad things happen to good cells.* Nat Rev Mol Cell Biol, 2007. **8**(9): p. 729-740.
3. Stewart, S.A. and R.A. Weinberg, *Senescence: does it all happen at the ends?* (0950-9232 (Print)).
4. Parrinello, S., et al., *Oxygen sensitivity severely limits the replicative lifespan of murine fibroblasts.* Nat Cell Biol, 2003. **5**(8): p. 741-747.
5. Hewitt, G., et al., *Telomeres are favoured targets of a persistent DNA damage response in ageing and stress-induced senescence.* Nat Commun, 2012. **3**: p. 708.
6. Lin, A.W., et al., *Premature senescence involving p53 and p16 is activated in response to constitutive MEK/MAPK mitogenic signaling.* Genes & Development, 1998. **12**(19): p. 3008-3019.
7. Kreiling, J.A., et al., *Age-associated increase in heterochromatic marks in murine and primate tissues.* Aging cell, 2011. **10**(2): p. 292-304.
8. Moiseeva, O., et al., *DNA Damage Signaling and p53-dependent Senescence after Prolonged β-Interferon Stimulation.* Molecular Biology of the Cell, 2006. **17**(4): p. 1583-1592.
9. Fagagna, F.d.A.d., et al., *A DNA damage checkpoint response in telomere-initiated senescence.* Nature, 2003. **426**(6963): p. 194-198.
10. de Lange, T., *Shelterin: the protein complex that shapes and safeguards human telomeres.* Genes & Development, 2005. **19**(18): p. 2100-2110.
11. Diotti, R. and D. Loayza, *Shelterin complex and associated factors at human telomeres.* Nucleus, 2011. **2**(2): p. 119-135.
12. Longhese, M.P., *DNA damage response at functional and dysfunctional telomeres.* Genes & Development, 2008. **22**(2): p. 125-140.
13. Maréchal, A. and L. Zou, *DNA Damage Sensing by the ATM and ATR Kinases.* Cold Spring Harbor Perspectives in Biology, 2013. **5**(9): p. a012716.
14. Herbig, U., et al., *Telomere Shortening Triggers Senescence of Human Cells through a Pathway Involving ATM, p53, and p21CIP1, but Not p16INK4a.* Molecular Cell, 2004. **14**(4): p. 501-513.
15. van Deursen, J.M., *The role of senescent cells in ageing.* Nature, 2014. **509**(7501): p. 439-446.
16. Ovadya, Y. and V. Krizhanovsky, *Senescent cells: SASPected drivers of age-related pathologies.* Biogerontology, 2014. **15**(6): p. 627-642.
17. Clapp, C., et al., *Expression of prolactin mRNA and of prolactin-like proteins in endothelial cells: evidence for autocrine effects.* Journal of Endocrinology, 1998. **158**(1): p. 137-144.
18. Acosta, J.C., et al., *Control of senescence by CXCR2 and its ligands.* Cell Cycle, 2008. **7**(19): p. 2956-2959.

19. Salminen, A., A. Kauppinen, and K. Kaarniranta, *Emerging role of NF-κB signaling in the induction of senescence-associated secretory phenotype (SASP).* Cellular Signalling, 2012. **24**(4): p. 835-845.
20. Freund, A., et al., *Inflammatory Networks during Cellular Senescence: Causes and Consequences.* Trends in molecular medicine, 2010. **16**(5): p. 238-246.
21. MD, B., *Genes and Disease.* Respiratory Diseases 1998.
22. Valavanidis, A., et al., *Pulmonary Oxidative Stress, Inflammation and Cancer: Respirable Particulate Matter, Fibrous Dusts and Ozone as Major Causes of Lung Carcinogenesis through Reactive Oxygen Species Mechanisms.* International Journal of Environmental Research and Public Health, 2013. **10**(9): p. 3886-3907.
23. MacNee, W., *Accelerated lung aging: a novel pathogenic mechanism of chronic obstructive pulmonary disease (COPD).* Biochemical Society Transactions, 2009. **37**(4): p. 819-823.
24. Lang, P.O., et al., *Immunological pathogenesis of main age-related diseases and frailty: Role of immunosenescence.* European Geriatric Medicine. **1**(2): p. 112-121.
25. Busse, P.J. and S.K. Mathur, *Age-related changes in immune function: Effect on airway inflammation.* Journal of Allergy and Clinical Immunology, 2010. **126**(4): p. 690-699.
26. association, A.L., *Trends in Asthma Morbidity and Mortality* 2016.
27. CDC(US), M.u.a., *A guide to health care professionals.* Global Initiative for Chronic Obstructive Lung Disease(GOLD) [Internet], 2011.
28. Mannino, D.M. and A.S. Buist, *Global burden of COPD: risk factors, prevalence, and future trends.* The Lancet. **370**(9589): p. 765-773.
29. (US), C.f.d.c., *Pocket guide for asthma management and prevention.* 2015.
30. Bartling, B., *Cellular senescence in normal and premature lung aging.* Zeitschrift für Gerontologie und Geriatrie, 2013. **46**(7): p. 613-622.
31. Heron, M., *A guide to health care professionals.* National Vital Statistics Reports, 2013. **65**(4).
32. HJ, M., *The remaking of chromosomes.* . Collecting Net, 1938;. **13**(181-198).
33. McClintock, B., *The Stability of Broken Ends of Chromosomes in Zea Mays.* Genetics, 1941. **26**(2): p. 234-282.
34. Coluzzi, E., et al., *Oxidative Stress Induces Persistent Telomeric DNA Damage Responsible for Nuclear Morphology Change in Mammalian Cells.* PLoS ONE, 2014. **9**(10): p. e110963.
35. Saretzki, G., et al., *Telomere shortening triggers a p53-dependent cell cycle arrest via accumulation of G-rich single stranded DNA fragments.* (0950-9232 (Print)).
36. Rode, L., et al., *Short telomere length, lung function and chronic obstructive pulmonary disease in 46 396 individuals.* Thorax, 2013. **68**(5): p. 429-435.
37. Munoz-Espin, D. and M. Serrano, *Cellular senescence: from physiology to pathology.* Nat Rev Mol Cell Biol, 2014. **15**(7): p. 482-496.
38. Fossel, M., *Use of Telomere Length as a Biomarker for Aging and Age-Related Disease.* Current Translational Geriatrics and Experimental Gerontology Reports **1**(2).
39. Belsky, D.W., et al., *Is Chronic Asthma Associated with Shorter Leukocyte Telomere Length at Midlife?* American Journal of Respiratory and Critical Care Medicine, 2014. **190**(4): p. 384-391.
40. Sadr, M., et al., *Telomere Shortening in Blood Leukocytes of Patients with Chronic Obstructive Pulmonary Disease.* Tanaffos, 2015. **14**(1): p. 10-16.
41. Ly, H., *Genetic and environmental factors influencing human diseases with telomere dysfunction.* International Journal of Clinical and Experimental Medicine, 2009. **2**(2): p. 114-130.
42. Takai, H., A. Smogorzewska, and T. de Lange, *DNA Damage Foci at Dysfunctional Telomeres.* Current Biology, 2003. **13**(17): p. 1549-1556.

43. Kuo, L.J. and L.-X. Yang, *γ-H2AX - A Novel Biomarker for DNA Double-strand Breaks.* In Vivo, 2008. **22**(3): p. 305-309.
44. Polo, S.E. and S.P. Jackson, *Dynamics of DNA damage response proteins at DNA breaks: a focus on protein modifications.* Genes & Development, 2011. **25**(5): p. 409-433.
45. Albrecht, E., et al., *Telomere length in circulating leukocytes is associated with lung function and disease.* European Respiratory Journal, 2014. **43**(4): p. 983-992.
46. Safdar, A., et al., *Aberrant Mitochondrial Homeostasis in the Skeletal Muscle of Sedentary Older Adults.* PLoS ONE, 2010. **5**(5): p. e10778.
47. Birch, J., et al., *DNA damage response at telomeres contributes to lung aging and chronic obstructive pulmonary disease.* American Journal of Physiology - Lung Cellular and Molecular Physiology, 2015. **309**(10): p. L1124-L1137.
48. Houben, J.M.J., et al., *Telomere shortening in chronic obstructive pulmonary disease.* Respiratory Medicine, 2009. **103**(2): p. 230-236.
49. Bricker, D.K., et al., *A Mitochondrial Pyruvate Carrier Required for Pyruvate Uptake in Yeast, Drosophila, and Humans.* Science, 2012. **337**(6090): p. 96-100.
50. Correia-Melo, C., et al., *Mitochondria are required for pro-ageing features of the senescent phenotype.* The EMBO Journal, 2016. **35**(7): p. 724-742.
51. Modica-Napolitano, J.S. and K.K. Singh, *Mitochondrial dysfunction in cancer.* Mitochondrion, 2004. **4**(5–6): p. 755-762.
52. Gray, L.R., S.C. Tompkins, and E.B. Taylor, *Regulation of pyruvate metabolism and human disease.* Cellular and Molecular Life Sciences, 2014. **71**(14): p. 2577-2604.
53. Chilosi, M., et al., *Premature lung aging and cellular senescence in the pathogenesis of idiopathic pulmonary fibrosis and COPD/emphysema.* Translational Research, 2013. **162**(3): p. 156-173.
54. Passos, J.F., et al., *Feedback between p21 and reactive oxygen production is necessary for cell senescence.* Molecular Systems Biology, 2010. **6**: p. 347-347.
55. Kyoh, S., et al., *Are leukocytes in asthmatic patients aging faster? A study of telomere length and disease severity.* Journal of Allergy and Clinical Immunology, 2013. **132**(2): p. 480-482.e2.
56. Wu, J., et al., *Central Role of Cellular Senescence in TSLP-Induced Airway Remodeling in Asthma.* PLoS ONE, 2013. **8**(10): p. e77795.
57. Michael, T., et al., *Calcium Sensing Receptor and Airway Reactivity in Mixed Allergen Treated Mouse Model of Asthma*, in *A29. INFLAMMATION AND MECHANISMS OF AIRWAY SMOOTH MUSCLE CONTRACTION*. 2016, American Thoracic Society. p. A1266-A1266.
58. Eltom, S., et al., *P2X7 Receptor and Caspase 1 Activation Are Central to Airway Inflammation Observed after Exposure to Tobacco Smoke.* PLoS ONE, 2011. **6**(9): p. e24097.
59. Nials, A.T. and S. Uddin, *Mouse models of allergic asthma: acute and chronic allergen challenge.* Disease Models & Mechanisms, 2008. **1**(4-5): p. 213-220.
60. Itoh, M., et al., *Systemic effects of acute cigarette smoke exposure in mice.* Inhalation Toxicology, 2014. **26**(8): p. 464-473.
61. de Carlos, S.P., et al., *Oxidative damage induced by cigarette smoke exposure in mice: impact on lung tissue and diaphragm muscle.* Jornal Brasileiro de Pneumologia, 2014. **40**(4): p. 411-420.
62. Agarwal, A.R., et al., *Short-term cigarette smoke exposure induces reversible changes in energy metabolism and cellular redox status independent of inflammatory responses in mouse lungs.* American Journal of Physiology - Lung Cellular and Molecular Physiology, 2012. **303**(10): p. L889-L898.
63. Jha, P. and R. Peto, *Global Effects of Smoking, of Quitting, and of Taxing Tobacco.* New England Journal of Medicine, 2014. **370**(1): p. 60-68.

64. Kim, C., et al., *Attenuation of Cigarette Smoke–Induced Emphysema in Mice by Apolipoprotein A-1 Overexpression.* American Journal of Respiratory Cell and Molecular Biology, 2015. **54**(1): p. 91-102.
65. Heidari, B., *The importance of C-reactive protein and other inflammatory markers in patients with chronic obstructive pulmonary disease.* Caspian Journal of Internal Medicine, 2012. **3**(2): p. 428-435.
66. Bartalesi, B., et al., *Different lung responses to cigarette smoke in two strains of mice sensitive to oxidants.* European Respiratory Journal, 2005. **25**(1): p. 15-22.
67. Schell, John C., et al., *A Role for the Mitochondrial Pyruvate Carrier as a Repressor of the Warburg Effect and Colon Cancer Cell Growth.* Molecular Cell, 2014. **56**(3): p. 400-413.
68. Stanley, S.E., et al., *Telomerase mutations in smokers with severe emphysema.* The Journal of Clinical Investigation. **125**(2): p. 563-570.
69. Dai, J., et al., *Telomerase gene mutations and telomere length shortening in patients with idiopathic pulmonary fibrosis in a Chinese population.* (1440-1843 (Electronic)).
70. Hoenicke, L. and L. Zender, *Immune surveillance of senescent cells—biological significance in cancer- and non-cancer pathologies.* Carcinogenesis, 2012.
71. Lujambio, A., *To clear, or not to clear (senescent cells)? That is the question.* Inside the Cell, 2016. **1**(2): p. 87-95.
72. Kay, M.M., *Mechanism of removal of senescent cells by human macrophages in situ.* Proceedings of the National Academy of Sciences of the United States of America, 1975. **72**(9): p. 3521-3525.
73. Bratosin, D., et al., *Cellular and molecular mechanisms of senescent erythrocyte phagocytosis by macrophages. A review.* Biochimie, 1998. **80**(2): p. 173-195.
74. Tumes, D.J., et al., *Strain-dependent resistance to allergen-induced lung pathophysiology in mice correlates with rate of apoptosis of lung-derived eosinophils.* Journal of Leukocyte Biology, 2007. **81**(6): p. 1362-1373.